ADVANCES IN INORGANIC CHEMISTRY, VOL. 38

REPLACEMENT OF SULFUR BY SELENIUM IN IRON–SULFUR PROTEINS

JACQUES MEYER,* JEAN-MARC MOULIS,* JACQUES GAILLARD,† and MARC LUTZ‡

* DBMS-Métalloprotéines, CENG 85X 38041 Grenoble, France
† DRFMC-SCPM, CENG 85X, 38041 Grenoble, France
‡ DBCM Biophysique des Protéines et des Membranes, CE-Saclay, 91191 Gif-sur-Yvette, France

I. Introduction

Selenium is a Group VIA element; it is in a bridging position in its column, lying between two nonmetals, oxygen and sulfur, and the increasingly metallic tellurium and polonium. In its period it lies between the metalloid arsenic and the halogen bromine. Se has six naturally occurring stable isotopes, ^{74}Se (0.87%), ^{76}Se (9.02%), ^{77}Se (7.58%), ^{78}Se (23.52%), ^{80}Se (49.82%), and ^{82}Se (9.19%), and several radioactive ones, including the γ emitter ^{75}Se ($t_{1/2}$ = 120 days), which is widely used as a tracer. ^{77}Se has a nuclear spin ($I = \frac{1}{2}$) and is increasingly used in nuclear magnetic resonance (NMR) studies (*1, 2*).

By its chemical properties, selenium is most similar to sulfur, and occurs in the same valence states, -2, 0, $+2$, $+4$, and $+6$. However, the two elements display noteworthy differences relevant to the biochemistry of selenium. Selenium tends to be more stable than sulfur in its intermediate oxidation states, and less stable in the extreme ones. Accordingly, selenate and selenite are relatively easy to reduce to the element, and selenides are more reactive (reducing) than sulfides. Selenium is most often found in biological systems in compounds such as selenols, diselenides, and selenoethers, which are usually more reactive than their sulfur counterparts, because of the greater polarity and lower strength of the C–Se, N–Se and O–Se bonds. Selenols are more acidic (usually ionized at neutral pH), are better nucleophiles, better leaving groups, and are more reducing than the corresponding thiols (*1, 2*).

The average concentration of selenium is ~0.1 ppm in the earth's crust, and three orders of magnitude lower in the oceans (*3, 4*). The biogeochemical cycle of selenium is similar to, but not coincident with, that of sulfur (*3, 4*). Selenium is used in electronics and metallurgy; in the glass and ceramics industry; in rubber, pigment, and explosive manufacture; and in some pharmaceuticals (reviewed in Ref. *2*).

II. Selenium in Biology

A. Selenium: A Toxic though Essential Element

Fatal horse and cattle diseases known as "blind staggers" and "alkali disease" were described in the Dakota Territory and neighboring states and territories in the 1850s, and were ascribed to selenium poisoning some 80 years later. Based on his description of 1295, Marco Polo came across similar diseases in his travels to China. Selenium has also been

labeled as carcinogenic, thus increasing the general feeling that it is a highly toxic and undesirable element (*5*). The subsequent demonstration of its essentiality (*6*), of human diseases associated with selenium deficiency (*7*), and of the presence of selenium in a number of biomolecules (*8*) has failed to reverse the mostly negative image of this element.

B. Selenium-Containing Biomolecules

Unlike animals, plants do not seem to require selenium and are less sensitive to the toxic effects of this element. In fact, some species of plants growing on selenium-rich soils accumulate considerable amounts (up to 0.5% of their dry weight) of this chalcogenide. In these plants selenium is stored in compounds that are metabolic dead ends, and is thus prevented from poisoning important processes (*9*).

Several enzymes have been demonstrated to contain selenium in the form of selenocysteine: formate dehydrogenases from *Escherichia coli,* glycine reductase from amino acid-fermenting clostridia, hydrogenases from *Methanococcus vannielii* and from *Desulfovibrio baculatus,* and mammalian glutathione peroxidase (*8*). Recent additions to this list are type I iodothyronine 5′-deiodinase from rat thyroid (*10, 11*) and a rat selenoprotein containing 10 UGA-encoded selenocysteines (*12*). Major advances have recently been made toward elucidation of the molecular mechanism by which selenocysteine incorporation takes place (*8*). This amino acid is encoded by UGA in all cases investigated so far (*8, 13, 14*). Selenocysteinyl-tRNA is formed by phosphorylation and subsequent selenylation of serine bound to a specific suppressor seryl-tRNA. Four genes, whose products are required for the incorporation of selenocysteine into proteins, have been identified in *E. coli.* These findings truly establish selenocysteine as the twenty-first amino acid (*8*).

A number of other selenoproteins, in which the status of selenium is still uncertain, have been reported. In most of these, neither the chemical form nor the specificity of selenium incorporation has been established (*15*). In the case of the thiolase from *Clostridium kluyveri,* selenomethionine is incorporated cotranslationally into the enzyme, in competition with methionine (*8*).

Selenium specifically occurs in tRNAs of some bacteria, plant cells, and mammalian cell lines. Bacterial seleno-tRNAs having glutamate- or lysine-accepting specificity contain 5-methylaminomethyl-2-selenouridine in the wobble position of the anticodons. The incorporation of selenium takes place by an ATP-dependent replacement of the sulfur atom of the corresponding thionucleoside (*8*).

In view of the numerous specific and well-characterized occurrences

of selenium in biomolecules, the essentiality of this element is obvious. Other possible beneficial effects of selenium are its working as an antioxidant or as a complexing agent of toxic heavy metals (*7*). In contrast, the well-known toxicity of selenium is less straightforwardly explained on a molecular basis. In fact, the replacement of sulfur by selenium is known to have little bearing on some coenzymes (*16*), and on the activity of the β-galactokinase from *E. coli* when substitution occurs on the methionine residues (*17*). The cysteine residues of proteins are a more critical target for selenium substitution, as they become more reactive and less stable. The toxic effect of selenium, which is often ingested as selenite, can also be exerted by the oxidative properties of the latter compound toward thiols: formation of disulfides or selenotrisulfides may result in the blocking of functionally essential cysteine residues (*4, 18, 19*).

C. Artificial Incorporation of Selenium into Proteins

As outlined above, selenium occurs in various biomolecules as a substitute for sulfur for the fulfillment of particular functions. Following this rationale, attempts have been made to artificially incorporate selenium into specific sites of proteins in order to modify their properties: the targets of these modifications have been cysteine or methionine residues, and the inorganic sulfur atoms of iron–sulfur proteins.

Selenocysteine has been introduced into the protease subtilisin by chemical modification of serine 221. The latter reaction was carried out by activating the hydroxyl group of the target residue with phenylmethylsulfonyl fluoride and subsequently treating the sulfonylated enzyme with a large excess of hydrogen selenide (*20*). Interestingly, the modification converted subtilisin into an acyltransferase with selectivity properties suitable for a peptide ligase (*20*), and into a glutathione peroxidase mimic (*20a*). A different approach, namely chemical synthesis of the whole polypeptide, was used to prepare several selenium analogs of small peptides or proteins, namely glutathione, oxytocin (*21*), somatostatin (*22*), and metallothionein (*23*). In the latter case, the substitution was aimed at obtaining structural information on the copper–chalcogenide cluster present in the protein.

Quantitative substitutions of methionine by selenomethionine in the copper protein azurin (*24*) and in ribonuclease H (*25*) were performed by growing methionine auxotrophic strains on selenomethionine.

Replacement of sulfide by selenide in the inorganic cores of iron–sulfur proteins will be treated in detail in the main body of this

review (see Table I for a summary on artificial replacement of sulfur by selenium in peptides and proteins).

D. Selenium as a Probe

As was discussed previously, the chemical properties of selenium are sufficiently similar to those of sulfur to allow replacement of the latter by the former in many biomolecules. However, the two elements differ significantly from each other by some of their physical characteristics, and for several methods of investigation selenium has proved to be a more efficient probe than sulfur.

The two chalcogens differ considerably in their atomic mass number A, selenium ($A = 79$) being more than twice as heavy as sulfur ($A = 32$). Accordingly, the replacement of S by Se is expected to considerably modify the vibrational properties of the substituted molecule. These selenium-induced changes have been instrumental in the analysis of resonance Raman spectra of iron–sulfur proteins (Section VIII).

Furthermore, the atomic mass of selenium qualifies it as a target for techniques that are impossible or difficult to perform with sulfur. In particular, selenium can be used as the absorbing atom for X-ray absorption spectroscopy; measurements on iron–selenium synthetic compounds have demonstrated the feasibility of the method (*26*), and recently it has been used to show that the coordination sphere of selenium in a hydrogenase from *D. baculatus* includes nickel and carbon (*27*). Selenium has also been used as an anomalous scatterer for phasing the X-ray diffraction data of ribonuclease H (*28*).

Another advantage of selenium is its possessing an isotope (^{77}Se) with nuclear spin $S = \frac{1}{2}$. When selenium atoms are involved in or near a paramagnetic center, enrichment with ^{77}Se results in electron paramagnetic resonance (EPR) spectra displaying hyperfine structures that can be resolved in some cases. This property has been implemented for several iron–sulfur proteins (Sections VI and VII), and has recently been used to confirm the involvement of selenocysteine in the nickel-containing active site of a hydrogenase from *D. baculatus* (*29*). Moreover, electron–nuclear double resonance (ENDOR) should in principle be possible with ^{77}Se, although no success has yet been reported. Finally, a probably even more promising application of ^{77}Se is its use in NMR: it provides adequate sensitivity (7×10^{-3} and 3 with respect to the proton and to ^{13}C, respectively) and a very wide chemical shift range (3000 ppm) (*2*). A considerable body of ^{77}Se NMR data has been gathered on a variety of synthetic compounds (*2*). The feasibility of NMR studies on selenium covalently or noncovalently attached to proteins

TABLE I

ARTIFICIAL INCORPORATION OF SELENIUM INTO PEPTIDES AND PROTEINS

Peptide or protein	Number of amino acids	Function	Site of selenium incorporation	Method	Reported results	Ref.
Subtilisin (*Bacillus subtilis*)	275	Protease	Conversion of Ser 221 into SeCys	Chemical modification	Conversion of enzyme into an acyltransferase and into a glutathione peroxidase mimic	*20, 20a*
Oxytocin	9	Hypophyseal hormone	Replacement of Cys 1 or Cys 6 by SeCys	Chemical synthesis	Subtle modifications of biological activity	*21*
Somatostatin	14	Inhibition of insulin secretion	Replacement of Cys 3 and Cys 14 by SeCys	Chemical synthesis	Functionally similar to native peptide	*22*
Metallothionein (*Neurospora crassa*)	25	Metal accumulation	Replacement of the seven Cys residues by SeCys	Chemical synthesis	UV-vis, CD, fluorescence	*23*
Azurin (*Pseudomonas aerogenes*)	128	Electron transfer	Replacement of the six methionine residues by SeMet	Growth of a methionine auxotroph on Se-methionine	Reduction potential, EPR, UV-vis spectra	*24*
Ribonuclease H (*E. coli*)	155	Degradation of RNA on DNA:RNA hybrids	Replacement of the four Met residues by SeMet	Growth of a methionine auxotroph on Se-methionine	Phasing of X-ray diffraction data	*25, 28*

Putidaredoxin (*Pseudomonas putida*)	106	Electron transfer in camphor oxidation	Inorganic sulfur atoms of [2Fe–2S] cluster	*In vitro* removal and reconstitution of Fe–Se cluster	Reduction potential, activity, UV-vis, EPR, Mössbauer	*35, 36, 81, 94, 96*
Adrenodoxin (beef adrenal glands)	114	Electron transfer in hormone hydroxylation	Inorganic sulfur atoms of [2Fe–2S] cluster	*In vitro* removal of native Fe–S and reconstitution of Fe–Se cluster	Reduction potential, activity, UV-vis, EPR, ENDOR, resonance Raman	*36, 38, 67, 82, 95, 96, 147*
Parsley ferredoxin	96	Electron transfer in photosynthesis	Inorganic sulfur atoms of [2Fe–2S] cluster	*In vitro* removal of native Fe–S and reconstitution of Fe–Se cluster	Reduction potential, UV-vis, CD, EPR	*37, 57, 96*
Spinach ferredoxin	97	Electron transfer in photosynthesis	Inorganic sulfur atoms of [2Fe–2S] cluster	*In vitro* removal of native Fe–S and reconstitution of Fe–Se cluster	UV-vis, resonance Raman	*48, 154*
Clostridial ferredoxins (*C. pasteurianum* and two other species)	55	Electron transfer in anaerobic metabolism	Inorganic sulfur atoms of [4Fe–4S] clusters	*In vitro* removal of native Fe–S and reconstitution of Fe–Se cluster	Reduction potential, activity, UV-vis, EPR, Mössbauer, MCD, resonance Raman, ^{1}H NMR	*39, 43, 49, 58, 59, 98–101, 153*
HiPIP (*Chromatium vinosum*)	85	Unknown	Inorganic sulfur atoms of [4Fe–4S] cluster	*In vitro* removal of native Fe–S and reconstitution of Fe–Se cluster	Reduction potential, UV-vis, EPR, resonance Raman, ^{1}H NMR	*40, 103*
Aconitase (beef heart mitochondria)	755	Isomerization of citrate	Inorganic sulfur atoms of [4Fe–4S] or of [3Fe–4S] cluster	*In vitro* removal of native Fe–S and reconstitution of Fe–Se cluster	Activity, EPR, Mössbauer	*41*

has been demonstrated (*30*) and recently confirmed with glutathione peroxidase containing ^{77}Se-enriched selenocysteine (*31*).

III. Preparation of Selenium-Substituted Iron–Sulfur Proteins

A. Historical Background

Soon after the discovery of ferredoxins (*32, 33*), it was shown that their active sites could be destroyed by acid and reconstituted *in vitro* (*34, 34a*). Several investigations were then carried out with selenide as a substitute for sulfide. The first studies were performed with the [2Fe–2S] proteins putidaredoxin (*35*), adrenodoxin (*36*), and parsley ferredoxin (*37*). A cobalt–selenium cluster has also been assembled in adrenodoxin (*38*). Successful substitutions have since been reported for [4Fe–4S] proteins: *Clostridium pasteurianum* ferredoxin (*39*), *Chromatium vinosum* high-potential ferredoxin (HiPIP) (*40*), and beef heart aconitase (*41*).

It had been observed early on that active site sulfide of *C. pasteurianum* ferredoxin could exchange with free sulfide at alkaline pH in the presence of urea, without complete denaturation of the protein (*42*). A similar exchange reaction with free selenide was later found in the same protein (*43*). It has also been demonstrated that iron and chalcogenide atoms are shuffled among synthetic analog molecules in solution (*44*). These reactions result in a random distribution of the chalcogenides in the metal clusters, and therefore cannot be used for the preparation of homogeneous selenium-substituted proteins. All such substitutions have so far invariably involved two steps: first, complete removal of the inorganic core of the active site, and then assembly of a new active site into the apoprotein.

B. Preparation of Apoproteins

For the preparation of a totally substituted protein in good yield, a prerequisite is the isolation of apoprotein completely devoid of iron and inorganic sulfur. When the conditions of iron–sulfur removal are not carefully controlled, zero-valent sulfur (mainly present as trisulfide bridges involving cysteine residues) remains attached to the apoprotein (*45*) and is subsequently reincorporated into the active site during the reconstitution reaction, together with the added chalcogenide. The resulting contamination is a serious problem when sulfur isotopes or

selenide are wanted in the active site (Section VIII). Although sulfur (0) can be removed from the apoprotein (*45, 46*), it is more convenient to set up conditions that yield S(0)-free apoprotein during the denaturation reaction.

1. Acid Denaturation

From our experience with several types of ferredoxins, we have deduced an experimental procedure applicable to most such proteins. The ferredoxin solution has to be brought to a concentration not exceeding 1 mg/ml and kept at ~0°C under a flow of inert gas prior to the addition of acid. During and after the addition of acid, stirring and inert gas flow should not be interrupted, thus allowing inorganic sulfur to escape as H_2S before it is oxidized. The reaction time is 30–60 min. Optimal conditions for the acid treatment are not the same for all proteins, and are therefore outlined below.

The preparation of apoproteins from plant [2Fe–2S] ferredoxins (*37, 47*) has been reexamined in detail (*48*), and the use of HCl (0.5–1 *M*) has been found to be essential for the isolation of clean apoprotein; trichloroacetic acid, which is often used in order to obtain other apoferredoxins, is not suitable here.

Sulfide-free apoproteins are usually easier to obtain with [4Fe–4S] than with [2Fe–2S] ferredoxins. The experimental conditions used for *C. pasteurianum* ferredoxin (*43*), namely treatment with 0.5 *M* trichloroacetic acid, can be extended to other ferredoxins of this family (*49*).

The isolation of apoproteins of high-potential [4Fe–4S] ferredoxins has proved more difficult than for the low-potential ones, most probably because of the larger size of the proteins and the limited accessibility of the cluster to reactants; complete removal of the inorganic core requires all the reactants to be kept in solution. This is achieved by bringing the protein solution to 5 *M* in guanidinium chloride before adding HCl to a final concentration of 0.5 *M*. After neutralization and dialysis, the apoprotein is precipitated with 0.5 *M* trichloroacetic acid (*40*).

2. Other Methods

For iron–sulfur proteins significantly larger than ferredoxins ($M_r >$ 20,000), the treatment with acid often yields irreversibly denatured apoprotein. A possible way out, which has only been implemented with ferredoxins (*34a*), would be to dissolve the precipitated protein in a chaotropic solvent (5–7 *M* guanidinium chloride, for instance), carry

out the reconstitution reaction in this solvent, and slowly eliminate guanidine by dialysis in oxygen-free conditions.

A different procedure, which has been used in the case of aconitase, consists in avoiding the acid denaturation altogether. The enzyme was treated with EDTA and ferricyanide until the chromophore was completely lost, and the apoprotein was subsequently separated from the other reactants by gel filtration (*50*).

Another possibility has been opened by the development of extrusion reactions (*51*) and by the separation of apoproteins from these reaction mixtures (*52*). However, the method is limited by the poor solubility of many of the larger iron–sulfur proteins in the mixed aqueous–organic solvents used for the extrusion reactions (*51, 53*). Thus, for proteins other than ferredoxins, the preparation of reversibly denatured apoproteins remains to be worked out in each particular case.

C. Assembly of Iron–Selenium Active Sites

The incorporation of iron–selenide active sites has been carried out by very similar procedures in all proteins, under experimental conditions based on those described for iron–sulfide clusters (*34*). Minor adjustments have been made in the pH and stoichiometry of the reagents (*43, 48*). The only difficulty arises from the low stability of selenide, as compared with sulfide: whereas the latter can be added as a commercial reagent (sodium sulfide, for example), selenide has to be prepared *in situ*.

Several ways of producing selenide have been elaborated: elemental selenium can be reduced by heating in a hydrogen atmosphere (*54*), by aluminum powder in aqueous ammonia (*55*), or by borohydride (*56*). An alternative consists in the straightforward reduction of selenite by thiols (*18, 19*). The latter procedure is convenient and is used most often (*37, 39, 40, 48*). We have observed that allowing selenite to react with the thiol (dithiothreitol is more effective than 2-mercaptoethanol) before adding the apoprotein resulted in higher yields (*48*) than adding selenite to the thiol–apoprotein mixture (*37*).

Stable selenium isotopes are often available only in the elemental state. They may be either first converted into selenite with nitric acid and then allowed to react with thiols (*37*), or reduced directly to selenide. The latter reaction was carried out with aluminum (*55*) in early studies (*35, 36*), but heating in a hydrogen atmosphere (*54*) has subsequently been preferred (*36, 48, 57, 58*). The same procedure has been implemented to reduce elemental sulfur to sulfide (*48, 58*). With both

chalcogenides, the best reconstitution yields have been obtained when the hydrogen–chalcogen reaction products were solubilized with a stoichiometric amount of dithiothreitol solution prior to the injection of the protein (*48, 58*).

Following the assembly of the Fe–S or Fe–Se active sites, a combination of anion-exchange chromatography (on DE-52 cellulose) and gel filtration (on Sephadex G-25) removes the excesses of inorganic reactants and of apoprotein (*48, 58*).

D. Assembly of Iron–Tellurium Active Sites

Because tellurium follows sulfur and selenium in the VIA group, one may expect it to be a potential substitute for these elements in iron–sulfur proteins, despite its increased metallic character. Following the successful incorporation of selenium, we attempted to prepare 2[4Fe–4Te] *C. pasteurianum* ferredoxin (*59*). A number of means were used to prepare telluride: reduction of tellurite with dithiothreitol and reduction of elemental tellurium with borohydride, with heated dihydrogen, or with sodium in liquid ammonia (*60*). No chromophore-containing protein could be isolated, either due to the lack of active site assembly or to the instability of the product. At that time, only one synthetic [4Fe–4Te]-containing compound ($Cs_7Fe_4Te_8$) had been synthesized in the solid state at a high (1050 K) temperature (*61*), and nothing was known about the stability of these species in solution. Incorporation of iron–tellurium clusters into bovine serum albumin had been claimed previously, but the experimental support was not compelling (*62*). Later, [4Fe–4Te] clusters with tellurolate (*63, 63a*) or thiolate (*64*) ligands were synthesized in solution, and the possibility of assembling such sites in proteins might be reevaluated. In any case, a low stability of the tellurated ferredoxin is to be expected, due to the high reactivity of telluride and to the larger size of the [4Fe–4Te] core (*63a, 64*), as compared to the native one. The decrease in active site stability observed upon Se/S substitution (*43*) is likely to be even larger upon Te substitution. In addition, all [4Fe–4Te] synthetic clusters reported so far have been isolated in the $[4Fe–4Te]^+$ oxidation state (*61, 63, 64*), and no evidence for reversible redox behavior has been provided. Extrapolation of these features to the active sites of proteins would constitute an additional destabilizing factor. Nevertheless, in view of the results obtained with the selenium-substituted ferredoxin, efforts aimed at the preparation of the tellurium analog would probably be rewarding.

IV. Mechanisms of Iron–Sulfur Cluster Assembly *in Vitro* and *in Vivo*

The mechanisms of metallocenter biosynthesis are currently under intense scrutiny (*65*). In comparison with other electron transfer proteins, cytochromes being a case in point, ferredoxins are remarkable in that their prosthetic groups do not, in principle, require complicated enzyme-catalyzed pathways for their biosynthesis. This property, together with particular features in their sequences, has led to the still widely accepted proposal that ferredoxins are probably the most primitive electron transfer proteins (*66*). The observation that the active sites of [4Fe–4S] ferredoxins assemble spontaneously when the reduced apoprotein is reacted with iron and sulfide (*34*) has been confirmed in numerous instances with many different ferredoxins, using selenide as well as sulfur (Section III,C). In addition, a given polypeptide chain strongly directs assembly toward its indigenous active site: attempts to incorporate alien centers into iron–sulfur apoproteins have only yielded very unstable products (*67, 68*). These data have suggested that, in ferredoxins at least, iron–sulfur centers might assemble *in vivo* by nonenzymatic reactions (*48, 66*).

The physiological significance of *in vitro* reconstitution reactions has been questioned upon finding that rhodanese would facilitate the assembly of [2Fe–2S] and [4Fe–4S] clusters in plant and *C. pasteurianum* ferredoxins, respectively (*69, 70*). However, the absence of rhodanese activity in *C. pasteurianum* appears to forbid any function of this enzyme in iron–sulfur cluster synthesis (*71*). Concerning plant ferredoxin, the improvement afforded by rhodanese was most likely due to the use of apoferredoxin containing significant amounts of sulfide, as witnessed by its UV-visible absorption in the 300- to 400-nm region (*69*). In our hands, the implementation of apoferredoxin deprived of any inorganic material allowed reconstitution reactions (*48*) at least as satisfactory as those reported with rhodanese (*69*).

A breakthrough in the understanding of iron–sulfur cluster assembly *in vivo* was apparently achieved with the discovery that chloroplasts contain an enzymatic activity allowing the use of cysteine sulfur as a source of sulfide for the [2Fe–2S] cluster of ferredoxin (*72*). More recently, however, the same group has reported that no more than a few percent of the labeled sulfide entered the ferredoxin [2Fe–2S] cluster, and that this incorporation was inhibited by the addition of nonradioactive sulfide (*73*). They have nevertheless found the Fe–S cluster formation to be ATP dependent, which might suggest an enzymatic process (*73*). In the present state of knowledge, no strong experimental evidence allows the rejection of a nonenzymatic process for the *in vivo* assembly of

at least some of the ferredoxin active sites: the main unsolved problem is the provision of sulfide (presumably in low concentrations) in the vicinity of the nascent or freshly synthesized polypeptide.

In the case of larger iron–sulfur proteins, which often contain more elaborate active sites than the ferredoxin ones, the involvement of ancillary proteins for the production of active enzymes is well established. One of the best known cases is nitrogenase, which catalyzes the reduction of dinitrogen to ammonia at the expense of ATP, and comprises two proteins, the Fe protein and the Mo–Fe (or V–Fe in some cases) protein (*74*). The molybdenum–iron cofactor of the Mo–Fe protein requires several proteins for its synthesis. The Fe protein, which contains a [4Fe–4S] cluster, also requires an additional protein (NifM) for its conversion into an active state, but it is not known whether NifM participates directly in the formation of the iron–sulfur cluster (*74*). Indirect evidence for enzymatic assembly of an Fe–S cluster has also been produced for the iron-only hydrogenase from *Desulfovibrio vulgaris;* upon expression in *E. coli,* this protein possesses its full complement of [4Fe–4S] clusters, but lacks its putative hydrogen-activating site, an iron–sulfur cluster of unknown structure. The latter can therefore be assumed to require for its biosynthesis an enzymatic system proper to the organisms producing this kind of enzyme (*75*).

Some proteins appear to stand on the borderline between those that can be reconstituted *in vitro* (most ferredoxins and aconitase; Section III,C) and those that definitely require additional enzymes for their conversion into active species (preceding paragraph). A case in point is the [2Fe–2S] ferredoxin from *C. pasteurianum* (*76*), which, upon reconstitution, yields a brown protein (the native one is red) having UV-visible (Fig. 1) and resonance Raman (Fig. 2) spectra different from those of the native one. The reconstituted protein does contain a conventional [2Fe–2S] cluster, but its iron content is twice as high as that of the native protein, in line with its larger absorbance in the UV-visible region (Fig. 1). Additional iron is thus present in other structures, the instability of which has so far impeded their full characterization (J. Meyer, J.-M. Moulis, J. Gaillard, and M. Lutz, unpublished results, 1984). Considering that the protein contains, in addition to the four cysteine ligands of the [2Fe–2S] cluster, one cysteine and three histidine residues, an additional cluster is possibly assembled during the reconstitution process, provided these potential ligands are appropriately positioned in the three-dimensional space. This, however, does not imply the operation *in vivo* of an enzymatic system for cluster assembly: the difference between the native and the reconstituted ferredoxin may result from different folding mechanisms occurring *in vivo* and *in vitro*.

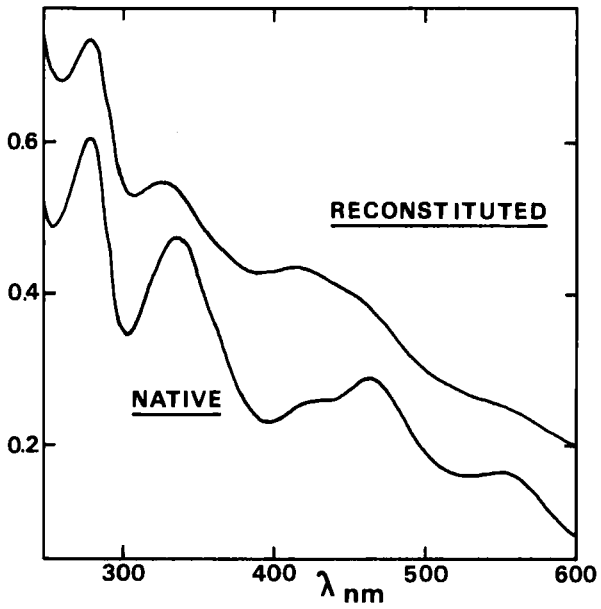

FIG. 1. UV-visible absorption spectra of native and reconstituted [2Fe–2S] *C. pasteurianum* ferredoxin. The native protein was purified as described (*76*). The reconstituted protein was prepared by the method (*48*) worked out for spinach ferredoxin. The path length was 1 mm and the protein concentrations were 7 mg/ml for the native one and 5 mg/ml for the reconstituted one. The difference spectrum (not shown) displays maxima at 300, 400, and 510 nm.

V. Biochemical Properties of Iron–Selenium Proteins

A. STABILITY

Selenium-substituted ferredoxins have consistently been found to be less stable than their native counterparts (*36, 37, 43*), in line with the intrinsically lower stability of the synthetic [4Fe–4Se] clusters, as compared to the [4Fe–4S] ones (*77*). A possible additional factor of instability in proteins is the larger size (*77, 77a*) of the [4Fe–4Se] cluster, which may therefore be less efficiently accommodated and protected by the polypeptide (*43*). We have measured the kinetics of solvolysis (*78*) of [4Fe–4S] and [4Fe–4Se] clusters in *C. pasteurianum* ferredoxin under oxygen-free conditions. The native protein was found not only to be more stable at neutral pH, but also to be stable over a much broader pH range than the selenium-substituted one (*43*). In addition, the selenium-substituted ferredoxins are more sensitive to oxidative

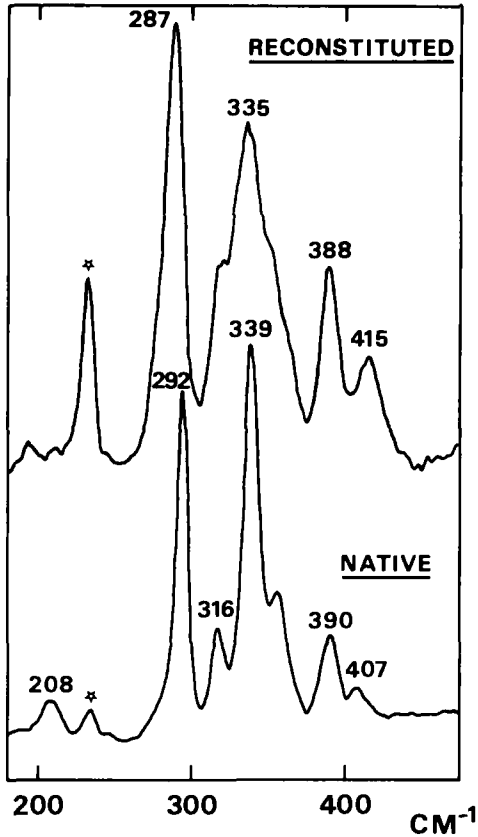

FIG. 2. Resonance Raman (RR) spectra, obtained with a 457.9-nm excitation wavelength, of native and of reconstituted [2Fe–2S] *C. pasteurianum* ferredoxin. The protein samples, which were those used in Fig. 1, were processed for RR data collection as described (*48, 153*). Other experimental conditions have been detailed elsewhere (*148, 153*). The starred bands at ~230 cm^{-1} arise from the Raman scattering of ice.

denaturation than the native ones (*43*), and should therefore systematically be handled under inert atmosphere.

B. UV-Visible Absorption Spectra

Replacement of sulfur by selenium in otherwise identical complexes has the general effect of decreasing ligand → metal charge transfer energy (*77, 77a*). Indeed, in selenium-substituted [2Fe–2S] proteins, the absorption bands at ~420 and 460 nm undergo red shifts of ~20

nm. In contrast, the ~330-nm band remains unchanged, which suggests that it arises mainly from (Cys)S → Fe charge transfer (*35, 36, 37, 48*). Similar shifts have been reported for synthetic analogs of binuclear active sites (*77a, 79*).

In [4Fe–4S] proteins the bathochromic shifts of the broad absorption bands at ~300 and 400 nm upon selenium substitution are hardly detectable (*43*) or are ill-defined (*40*). The main cause of this small effect is that these transitions involve overlapping S(e)* → Fe and (cys)S → Fe charge transfers. Similar observations have been reported for synthetic water-soluble clusters having aliphatic thiolate ligands (*43*). Well-characterized red shifts have only been observed in [4Fe–4S(e)] clusters having aromatic ligands: in this case, the shifts were larger when the substitution was carried out on the terminal organic ligands (20 nm) than when carried out on the bridging inorganic ones (8–13 nm) (*77, 80*), as expected for clusters having predominantly RS → Fe transitions near their visible absorption maxima at ~450 nm (*58*).

C. Redox Potentials

The replacement of sulfur by selenium in homologous coordination complexes most often results in positive reduction potential shifts (*77, 77a*). The same holds true for synthetic analogs of [2Fe–2S] (*79*) and [4Fe–4S] active sites (*77*), with positive shifts in the 0- to 60-mV range. In proteins, the reduction potential shifts have similar magnitudes, but are more variable in sign: shifts of +38 mV (parsley ferredoxin) (Ref. *57*), −10 mV (putidaredoxin) (Ref. *81*), and −14 mV (adrenodoxin) (Ref. *82*) have been reported for [2Fe–2S] proteins, and shifts of +6 mV (*C. pasteurianum* ferredoxin) (Ref. *43*) and −65 mV (*C. vinosum* HiPIP) (Ref. *40*) have been reported for [4Fe–4S] proteins. These apparent inconsistencies may arise in part from the lack of accuracy of the measurements, but the effect of the polypeptide chain, which is different in each case, probably plays a role as well. It should be kept in mind that the $[4Fe–4S]^{2+/+}$ active sites, for example, cover an ~300-mV range of reduction potentials, depending on the protein in which they are accommodated (*83*). A number of parameters, including solvent accessibility and networks of hydrogen bonds surrounding the active sites, are likely contributors to the adjustment of the redox properties of the iron–sulfur clusters in proteins. The balance between these effects remains ill-defined and is likely to vary from one protein to another. For instance, the hydrogen bonds involving chalcogenide atoms proba-

bly differ in various proteins, but are also likely to be modified in different ways upon Se/S substitution.

D. Enzymatic Activity

The only true iron–sulfur enzyme in which sulfide has been replaced by selenide is aconitase. Its activity with isocitrate as the substrate is enhanced upon selenium substitution (*41*). In ferredoxins of known function, the selenium-substituted proteins are only marginally different from their native counterparts in their ability to exchange electrons with their redox partners (*35–37, 43*). In the case of the electron transfer from the 2[4Fe–4S(e)] ferredoxin to hydrogenase I from *C. pasteurianum,* the selenium-substituted ferredoxin has a lower maximum velocity and a lower K_m than its native counterpart (*43*).

VI. Magnetic Properties of Iron–Selenium Clusters

Ferredoxins and other iron–sulfur proteins containing simple clusters are characterized, in their paramagnetic states, by a fast-relaxing EPR signal observed at low temperatures (usually between 4 and 100 K) in the $g = 2$ region. This property led to the discovery of these proteins (*84*) and to the deduction of the essential structural elements of the [2Fe–2S] site (*85, 86*). Besides EPR, the techniques used most often for monitoring the magnetic properties of iron–sulfur clusters are Mössbauer spectroscopy (*87*) and magnetic circular dichroism (MCD) (*88*). A unique position is held by ^{1}H NMR, which can use the protons neighboring the metal centers as probes of their magnetic state in liquid solution (*89*).

A. [2Fe–2S(e)] Proteins

In the $[2Fe–2S(e)]^{2+}$ redox level, these proteins are diamagnetic due to the strong antiferromagnetic coupling between the two Fe(III) ions. Upon reduction, the added electron is localized on one of the iron atoms, and the ground spin state of the antiferromagnetically coupled system has invariably been found to be $S = \frac{1}{2}$ (*90, 91*), even in those cases in which partial nonsulfur ligation is believed to occur (*92*).

The replacement of sulfide by selenide in adrenodoxin has allowed an unequivocal demonstration that two inorganic chalcogenide atoms are involved in the binuclear iron–sulfur sites. This has been inferred from the hyperfine structure appearing in the low-field component of

the EPR spectrum of samples enriched with ^{77}Se ($I = \frac{1}{2}$) (*36*). In contrast, ^{33}S ($I = \frac{3}{2}$) produced only line broadening and could not be used for a quantitative evaluation.

In all cases investigated so far, including a number of synthetic analogs (*93*), the replacement of sulfide by selenide has resulted in a general shift of the EPR spectra to a lower field (*35–37*). Concerning the symmetry of the *g* tensor, the effects of selenium substitution are more variable: in the case of putidaredoxin, the axial spectrum of the native protein is converted into a rhombic one (*35*), whereas in the case of parsley ferredoxin, the rhombic spectrum of the native protein is converted into one nearer to axial symmetry (*37*). Comparison of native and [2Fe–2Se] putidaredoxin by Mössbauer spectroscopy has shown that the hyperfine coupling constants and the isomer shifts of the iron atoms are slightly decreased in the Se-substituted protein (*94*). Similar results and conclusions have been reached by ^{57}Fe and proton ENDOR spectroscopy of native and Se-substituted adrenodoxin, with different effects, however, on the Fe(III) and on the Fe(II) sites (*95*). These variations have been interpreted as being similar to those observed among native [2Fe–2S] proteins (*96*).

In ^{1}H NMR spectra of synthetic binuclear iron–sulfur clusters, the isotropic shifts of the protons of the thiolate ligands increase slightly when sulfide is replaced by selenide, in both the oxidized (*77a, 79*) and the reduced (*44*) state. No data of this kind are available for [2Fe–2S(e)] proteins.

B. [4Fe–4S(e)] Proteins

Tetranuclear iron–sulfur clusters are diamagnetic at low temperature in the $[4Fe–4S]^{2+}$ redox level, and are paramagnetic ($S = \frac{1}{2}$; but see Section VII) either in the $[4Fe–4S]^{+}$ (reduced low-potential ferredoxins) or $[4Fe–4S]^{3+}$ (oxidized HiPIP) redox levels (*87*). The replacement of sulfide by selenide in $[4Fe–4S]^{2+}$ centers results in changes qualitatively similar to those described above for [2Fe–2S] clusters. The resonances of the protons neighboring the iron–sulfur cluster are consistently shifted to lower field upon replacement of sulfide by selenide, in synthetic analogs (*44, 97*) as well as in proteins (*98*). The intensity of the MCD spectra is greater for Se-substituted *C. pasteurianum* ferredoxin than for its native counterpart (*99*). The Mössbauer isomer shifts of the Se-substituted protein are slightly larger than those of the native protein (*100, 101*). A similar change has been observed in aconitase (*41*).

Similar variations in MCD (*99*), and ^{1}H NMR (*44, 97*) spectra have

been observed for $[4Fe–4S(e)]^+$ clusters upon replacement of sulfide by selenide, in those cases in which the ground spin state is $S = \frac{1}{2}$. The EPR spectra in the $g = 2$ region are slightly shifted to lower field (*49, 77, 100*), as observed for $[2Fe–2S(e)]^+$ clusters (Section VI,A). The ^1H NMR spectra of $[4Fe–4S]^+$ synthetic clusters with C_6H_5XH (X = S, Se, Te) terminal ligands display increasingly shifted proton NMR resonances when going downward in the row of the VIA elements (*64*).

For the $[4Fe–4Se]^{3+}$ redox level, the only available data are those concerning the oxidized HiPIP from *C. vinosum*. The EPR spectra are shifted to lower field in this case as well and are more anisotropic than those of the native protein (*40*). Whereas no low-field signals suggestive of $S > \frac{1}{2}$ ground spin states have been detected, the occurrence of several signals in the $g = 2$ region may arise from the existence of more than one $S = \frac{1}{2}$ ground spin state (*40, 102*). The shifted proton resonances occur at slightly lower field in NMR spectra of the Se-substituted protein than in those of the native one (*103*; J.-M. Moulis and J. Gaillard, unpublished results, 1987). Some of the latter results have been obtained with the HiPIP of a most interesting chimeric organism, combining, if not the properties, at least the names of anaerobic heterotrophs and purple sulfur bacteria, *"Clostridium vinosum"* (*103*).

C. [3Fe–4S(e)] Proteins

The only reported case of selenium incorporation into a trinuclear cluster is that of inactive aconitase (*41*). The EPR spectrum of the $[3Fe–4Se]^+$ protein ($S = \frac{1}{2}$) is not shifted to low field, but displays a significant increase in g tensor anisotropy, as compared to the $[3Fe–4S]^+$ protein (*41*). The Mössbauer spectra of the two species in this redox level witness slight differences in hyperfine parameters and larger anisotropies in the Se-substituted protein than in the native one. Upon reduction to $[3Fe–4S(e)]^0$, the Mössbauer spectra of the two proteins are nearly identical (*41*).

VII. Ground Spin State Variability in $[4Fe–4S(e)]^+$ Clusters

The spin-coupling model resulting in a $S = \frac{1}{2}$ ground state (*87*) has long been considered to be valid for all $[4Fe–4S(e)]^+$ clusters. Exceptions to the normally expected spectroscopic signature were few: the low-field EPR features of some synthetic analogs in the solid state (*104, 104a*) (Section VII,C), the so-called P-clusters of the nitrogenase Mo–Fe

protein (*105*) (Section VII,D,1), and the phosphoribosylpyrophosphate amidotransferase from *Bacillus subtilis* (*106*) (Section VII,D,2). These observations became more meaningful upon analysis of the unusual features displayed by the EPR and Mössbauer spectra of reduced Se-substituted clostridial ferredoxins, and the subsequent unveiling of analogous spin states in a number of other proteins.

A. Clostridial 2[4Fe–4Se]$^+$ Ferredoxins

Reduced Se-substituted clostridial ferredoxins display EPR features in the $g = 2$ region that are not unlike those observed for their native counterparts. Upon partial (<20%) reduction, the proportion of molecules containing two reduced clusters is negligible, and $S = \frac{1}{2}$ spectral features are observed (Section VI,B), with a slight shift to lower field in the case of the Se-substituted proteins (*100*). Upon full reduction, the native ferredoxins have long been known to display a seven-line spectrum arising from the interaction of two $S = \frac{1}{2}$ systems (*107*). In contrast, in 2[4Fe–4Se]$^+$ proteins, the interaction is reflected in a mere broadening of the spectra (*49, 100*). Whether this is due to specific properties of the $S = \frac{1}{2}$ spin states in [4Fe–4Se]$^+$ clusters or to the superimposition of spectral components involving interactions among various spin states (see below) remains to be determined.

Downfield of the $S = \frac{1}{2}$ signals, 2[4Fe–4Se]$^+$ clostridial ferredoxins display unusual features that have counterparts in the Mössbauer spectra (*100*); these have been assigned to $S = \frac{3}{2}$ and $S = \frac{7}{2}$ ground spin states (*49, 100, 101*). Low-temperature MCD spectra of these proteins are much more intense than those of their native counterparts, and their magnetization curves confirm the coexistence of $S > \frac{1}{2}$ ground spin states (*99*).

1. $S = \frac{3}{2}$ Spin State

Besides the signal corresponding to the $S = \frac{1}{2}$ species, the EPR spectra of 2[4Fe–4Se]$^+$ clostridial ferredoxins are dominated by a broad, fast-relaxing feature around $g = 4$. It is sensitive to cluster–cluster magnetic interaction, since, in the partially reduced proteins, it is resolved into two lines with g values of 4.5 and 3.5 (*100*). As it spreads into the $g = 2$ region, it has been described by a rhombic g tensor with principal values, 4.5, 3.5, and 2, and attributed to the $\pm\frac{1}{2}$ fundamental doublet of a spin quartet state with $|E/D| = 0.08$ (*100*), D being the zero-field splitting constant and E the rhombic distortion parameter. Additional information has been gathered from the Mössbauer spectra; after subtracting the contributions from the $S = \frac{1}{2}$ and $S = \frac{7}{2}$ (Section VII,A,2)

spin systems, the low-temperature spectra of 2[4Fe–4Se]$^+$ *C. pasteurianum* ferredoxin recorded under very strong applied fields (5–10 T) reveal that the iron sites experience a quasi-isotropic hyperfine tensor of small negative principal values. Moreover, the iron sites appear to be identical, although some inequivalence may be hidden under the breadth of the lines (*101*). From the shape of the Mössbauer spectra at intermediate applied fields, D has tentatively been estimated to be smaller than $+3$ cm^{-1}. All of these characteristics clearly distinguish the species giving rise to the $S = \frac{3}{2}$ state from those generating $S = \frac{1}{2}$ spin systems. Spin states closely resembling the one described above have been identified in a number of [4Fe–4S]$^+$ clusters, including those occurring in natural proteins (Sections VII,B–VII,D).

2. $S = \frac{7}{2}$ Spin State

The $\frac{7}{2}$ spin state, which has not yet been observed in any *bona fide* [4Fe–4S(e)]$^+$ clusters other than those of clostridial ferredoxins (*77a*), has been detected in the EPR and Mössbauer spectra of the latter proteins as very characteristic features (*49, 100, 101*). In fact, all sublevels of this octet spin system have been observed by a combination of these two spectroscopic techniques. The fundamental Kramers' doublet is very anisotropic, as indicated by its calculated g values (14.3, ~0, ~0), and can only be observed in the low-temperature (below ~15 K) Mössbauer spectra, even without applied magnetic fields (*100*). It is observed, on both sides of the central doublet, as a doublet of lines arising from two antiferromagnetically coupled species in a 3 : 1 intensity ratio. It can be described, to a first approximation, by a very simple model involving three ferromagnetically coupled Fe(II) ions, antiferromagnetically coupled with a single Fe(III) ion (*101*). At least one component of each of the excited levels has been observed by EPR (*49*); signals at $g = 10.08$, $g = 5.17$, and $g = 12.88$ have been assigned to the $\pm\frac{5}{2}$, $\pm\frac{3}{2}$, and $\pm\frac{1}{2}$ Kramers' doublets, respectively, of the $S = \frac{7}{2}$ state, with $D = -2$ cm^{-1} and $|E/D| = 0.12$. These characteristics suggest that the species giving rise to the $S = \frac{7}{2}$ spin state experiences forces that strongly tend to localize the electrons on the iron sites, a rather uncommon feature for [4Fe–4S(e)]$^+$ clusters.

3. Comments

At the time of their initial characterization in [4Fe–4Se]$^+$ clostridial ferredoxins (*100*), the novelty of the $S = \frac{3}{2}$ and $S = \frac{7}{2}$ spin states might have raised some doubts as to their being associated with tetranuclear Fe–S(e) clusters. A comprehensive set of chemical, biochemical (*43*), and spectroscopic (resonance Raman and Mössbauer) (*58, 100*) data was

therefore collected, providing ample evidence that all the iron in these proteins is present in $[4Fe–4Se]^{2+/+}$ clusters.

The coexistence of three ground spin states in proteins containing only two [4Fe–4Se] clusters forbids the assignment of a given spin state to a specific cluster. By combining integration of EPR spectra and fitting of Mössbauer spectra, we have been able to show that the proportion of $[4Fe–4Se]^{+}$ clusters assuming a given spin state is invariable in different preparations of the same protein, but variable as a function of the ferredoxin used (*C. pasteurianum, Clostridium acidiurici,* and *Clostridium thermosaccharolyticum*) (*49*). These results point to the essential role, in the present case, of the polypeptide chain in determining the forces giving rise to the ground spin state variability, and to the minor role, if any, of extrinsic factors such as sample processing or solvent composition. Further evidence of the paramount importance of the protein is provided by the observation that in Se-substituted *Bacillus stearothermophilus* ferredoxin only the $S = \frac{1}{2}$ ground spin state has been observed (*49*). The fact that the latter protein contains only one $[4Fe–4Se]^{+}$ cluster might suggest that the ground spin state variability in clostridial ferredoxins arises from magnetic interactions between the two clusters present in these proteins. This possibility is excluded by the observation that the high-spin multiplets occur in partially reduced clostridial ferredoxins as well (*100*). In fact, the magnetic interaction between the two clusters can be observed, not only on the EPR signal of the $S = \frac{1}{2}$ spin state, but also on that of the $S = \frac{3}{2}$ spin state (Section VII,A). In contrast, the $g = 5.17$ EPR line (attributed to the $\pm\frac{3}{2}$ Kramers' doublet of the $S = \frac{7}{2}$ state) appears to be insensitive to the interaction between the two clusters (*100*).

The ground spin state variability of tetranuclear iron–sulfur clusters has been analyzed in detail in two other cases, the nitrogenase iron protein (Section VII,B) and a series of synthetic analogs (Section VII,C). These studies have prompted a number of searches for similar properties (Section VII,D), and the general occurrence of ground spin state variability in $[4Fe–4S(e)]^{+}$ clusters is now widely recognized (Sections VII,B–VII,D; see Table II).

B. Nitrogenase Iron Protein

The Fe protein is the smaller (~60 kDa) component of nitrogenase, and is a dimer of two identical subunits (*74*). It contains a [4Fe–4S] cluster, which in the reduced state displays an $S = \frac{1}{2}$-type EPR spectrum (*74, 108*). Integration of the latter, however, has without exception yielded less than 0.5 spin/molecule, which has led to various hypotheses

on the active site structure (reviewed in Ref. *109*). The early observation of low-field EPR features in the $g = 4–5$ region (*110*) has long been overlooked. It has eventually been demonstrated, upon analysis of a comprehensive set of EPR, Mössbauer, and magnetic susceptibility data, that the $[4Fe–4S]^+$ cluster of the Fe protein exhibits a mixture of $S = \frac{1}{2}$ and $S = \frac{3}{2}$ spin states (*109*). The $S = \frac{3}{2}$ state is characterized by $D = -2.5\ cm^{-1}$, $|E/D| = 0.22$, and by weak and negative magnetic hyperfine interactions (*109*). The latter property has been observed for the $S = \frac{3}{2}$ state of $2[4Fe–4Se]^+$ ferredoxins as well (Section VII,A,1). Interconversions between the two spin states occur upon changes in solvent composition: in 50% ethylene glycol most of the clusters are in the $S = \frac{1}{2}$ state, whereas in 0.4 *M* urea the $S = \frac{3}{2}$ state predominates (*109*). The complexity of the electronic structure of the $[4Fe–4S]^+$ cluster in nitrogenase Fe protein is further illustrated by the effects of adenine nucleotide binding; the EPR and Mössbauer data again indicate the coexistence of $S = \frac{1}{2}$ and $S = \frac{3}{2}$ states, but they are not identical with those of the native protein. In addition, minor features in the spectra suggest the occurrence of an $S = \frac{5}{2}$ spin state in the ATP-bound Fe protein (*111*). Although the main characteristics of the Fe protein electronic structure have been worked out with the protein from *Azotobacter vinelandii* (*109, 111, 112*), equivalent features have been reported for the Fe proteins purified from *Klebsiella pneumoniae, Azotobacter chroococcum* (*113*), and *C. pasteurianum* (*114, 115*).

C. Synthetic Analogs

Synthetic analogs are structural and electronic representations of isoelectronic protein sites, where thiolate ligands simulate cysteinate binding in proteins (*116*). One of the significant advantages of these compounds, as compared with proteins, is the potential to obtain highly accurate tridimensional structures.

Initial observations of low-field features in EPR spectra of $[4Fe–4S]^+$ in the solid state (*104, 104a*) have subsequently been extended to show that $S = \frac{3}{2}$ ground spin states are exhibited by some of these clusters either in the solid state or in frozen solution (*117*). A wide survey of many $[4Fe–4S(e)]^+$ compounds in the polycrystalline state has revealed that those possessing a pure $S = \frac{1}{2}$ or $\frac{3}{2}$ spin state are a minority, and that most of them exhibit mixtures of these two spin states, or even spin admixed states. The latter are distinct from physical mixtures of $S = \frac{1}{2}$ and $S = \frac{3}{2}$ states, and possess properties intermediate between those of the pure states (*118*). When dissolved and frozen in acetonitrile or in *N,N*-dimethylformamide (DMF), however, all of these clusters

TABLE II

GROUND SPIN STATES OF $[4Fe–4S(e)]^+$ CLUSTERS

Compound	Ground spin state properties	Ref.
Synthetic $[Fe_4S(e)_4(SR)_4]^{3-}$ clusters	*In crystalline state,* three categories: pure $S = \frac{1}{2}$ or $S = \frac{3}{2}$, physical mixture of $S = \frac{1}{2}$ and $S = \frac{3}{2}$, spin admixed ($S = \frac{1}{2} + \frac{3}{2}$) *In frozen solution,* always a physical mixture of $S = \frac{1}{2}$ and $S = \frac{3}{2}$; relative proportion of $S = \frac{3}{2}$ state tends to increase with bulkiness of ligand	*77a, 104a, 104, 117–120*
$2[4Fe–4Se]^+$ clostridial ferredoxins	Three coexistent ground spin states: $S = \frac{1}{2}$, $S = \frac{3}{2}$, $S = \frac{7}{2}$; their relative proportions depend only on polypeptide chain, not on extrinsic parameters (solvent composition, freezing conditions) High-spin states contribute to the magnetic properties in solution at room temperature	*49, 59, 98–101*
Nitrogenase iron protein	Two coexistent spin states: $S = \frac{1}{2}$, $S = \frac{3}{2}$; their relative proportions depend on extrinsic parameters (solvent composition, freezing conditions (Fig. 3). Upon ATP or ADP binding, a different type of $S = \frac{3}{2}$ state appears; ATP binding causes the appearance of an $S = \frac{5}{2}$ state No contribution of the $S > \frac{1}{2}$ states is observed in solution at room temperature	*109, 111–115*

Nitrogenase Mo–Fe protein (P-clusters)	An $S = \frac{7}{2}$ ground spin state is observed, but only upon addition of solid thionine in large excess Note: the P-clusters have not been conclusively demonstrated to assume a [4Fe–4S] structure	*121–125*
Glutamine phosphorybosyl-pyrophosphate amidotransferase	$S = \frac{3}{2}$ is the predominant ground state, $S = \frac{1}{2}$ and $S = \frac{5}{2}$ are also observed; $S = \frac{5}{2}$ becomes dominant at high protein concentrations	*106, 126–129*
Pyrococcus furiosus ferredoxin	$S = \frac{1}{2}$ and $S = \frac{3}{2}$ states, the latter one being predominant; relative proportions nearly independent of solvent composition The [4Fe–4S] cluster has only three cysteine ligands; upon cyanide binding, only $S = \frac{1}{2}$ is observed	*130, 131*
Desulfovibrio africanus ferredoxin III	$S = \frac{1}{2}$ and $S = \frac{3}{2}$	*132, 133*
C. pasteurianum hydrogenase I (F-clusters)	$S = \frac{1}{2}$ and $S = \frac{3}{2}$	*134*
Clostridium thermoaceticum CO dehydrogenase	$S = \frac{1}{2}$ and $S = \frac{3}{2}$	*135*

display physical mixtures of $S = \frac{1}{2}$ and $\frac{3}{2}$ states (*118*). In frozen solution, the proportion of $S = \frac{3}{2}$ state increases roughly with the steric size of the thiolate ligand (*118*). Extensive crystallographic work has been carried out on these compounds, in an attempt to correlate structure and spin state. Several kinds of distortions have been evidenced in these studies performed at ambient temperature, but no unique core distortion or thiolate ligand conformation can be associated with any of the spin states observed at cryogenic temperature (*77a, 119, 120*).

D. Other Proteins

1. Nitrogenase Mo–Fe Protein

This protein is the larger component of nitrogenase. It contains 30–32 Fe and 2 Mo atoms per $\alpha_2\beta_2$ tetramer ($M_r \sim 230{,}000$). The Mo–Fe protein possesses two identical cofactors of approximate composition $MoFe_{6-8}S_{8-10}$, which are the probable catalytic centers. The remaining iron atoms belong to structures, referred to as "P-clusters," which have long been considered, but not proved, to be [4Fe–4S] centers (*74, 108, 116*). According to recent X-ray diffraction data, the P-clusters would appear to consist of two closely associated [4Fe–4S] clusters, or of a larger type of iron–sulfur cluster (*120a*). Most of the current knowledge on the P-clusters has been obtained from Mössbauer experiments that revealed coupled iron sites compatible with [4Fe–4S] structures (*105, 108, 116*). A particularly interesting study has been carried out on a protein having P-clusters specifically enriched in ^{57}Fe, and which did therefore not require subtraction of the contributions of the Mo–Fe cofactors (*121*).

In the Mo–Fe protein as isolated, the P-clusters (P^N) are diamagnetic in their ground state. Upon one-electron oxidation (P^{OX}), they are split into two subpopulations (each consisting of antiferromagnetically coupled iron sites in a 3 : 1 ratio) that differ only in the parameters of their minor component. Despite this difference, both subsets have $S > \frac{1}{2}$ noninteger spin states (*121*), in agreement with previous low-temperature MCD (*122*) and room temperature magnetic susceptibility (*123*) measurements. However, the spin multiplet could not be identified unambiguously, since only the ground doublet had been detected in the Mössbauer spectra (*121*). In another study, large excesses of solid thionine have been found to generate EPR signals at $g = 10.4$, 5.8, and 5.5; these have been attributed to the excited sublevels of a $S = \frac{7}{2}$ spin state with $D = -4\ cm^{-1}$ and $E = 0.16\ cm^{-1}$ (*124*). These spectra have arbitrarily been assigned to the P^{OX} state, and two speculative models

have been proposed to represent the redox reactions of the P-clusters (*124*). Subsequent Mössbauer studies of samples oxidized with solid thionine have proved that a P^{OX} ($S = \frac{7}{2}$) state is generated, but that it is different, though isoelectronic, from the previously studied P^{OX} state (*125*). The former lacks the trapped-valence Fe(II) site characteristic of the latter. Upon removal of the solid dye, the P^{OX} ($S = \frac{7}{2}$) state disappears and reverts to the classical P^{OX} state (*125*). The evidence presented strongly suggests that the $S = \frac{7}{2}$ state results from the interaction of the protein with the solid dye and that this state does not satisfactorily describe the spin states of the oxidized P-clusters in solution, in particular during the catalytic cycle (*125*). Concerning the latter point, it remains to be established that the P^{OX} state bears any relevance to the catalytic cycle of nitrogenase, since the available evidence rather suggests that the Mo–Fe protein requires reduction of the "as-isolated" level before passing on electrons to the substrates (*74, 108*).

Definite problems remain unresolved concerning the P-clusters, mainly due to their differing in many properties from well-characterized [4Fe–4S] clusters. If they are demonstrated to possess the latter structural framework, their terminal ligation pattern may have to differ from the classical one (one cysteine per iron), in order to simultaneously accommodate all of their known properties (*116*).

2. *Glutamine Phosphoribosylpyrophosphate Amidotransferase (GPRPAT)*

This enzyme catalyzes the replacement of the pyrophosphate group of 5-phosphoribosyl-1-pyrophosphate by the amide amino group of glutamine, the first step in purine nucleotide biosynthesis. The enzyme purified from *B. subtilis* contains a [4Fe–4S] cluster essential for activity, and is one among an increasing number of iron–sulfur enzymes that are not involved in redox reactions (*126*). The cluster has been suggested to work as an oxygen sensor, but whether it undergoes redox transitions *in vivo* remains undetermined (*127*). The enzyme can be partially reduced *in vitro* to the $[4Fe–4S]^{+}$ level, quantitative reduction being difficult because of its unusually low (-600 mV) reduction potential (*106*). Mössbauer spectra of the reduced enzyme have pointed to a half-integer ground spin state with a very anisotropic fundamental doublet, resulting in almost undetectable EPR spectra (*106*). MCD data have suggested an $S = \frac{3}{2}$ ground spin state with axial symmetry and $D > 3\,cm^{-1}$ (*128*). Furthermore, EPR signals consistent with transitions within the $\pm\frac{1}{2}$ Kramers' doublet of the $S = \frac{3}{2}$ spin state have been detected at low field, together with additional signals attributable to

$S = \frac{1}{2}$ and $S = \frac{5}{2}$ spin states (*128*). If these species are truly associated with $[4Fe–4S]^+$ clusters, which remains to be demonstrated, it is interesting that the $S = \frac{5}{2}$ spin state increases in abundance with protein concentration (*128*). Since GPRPAT has been shown to be a mixture of monomers, dimers, and tetramers in solution (*129*), the spin state variability of the cluster has tentatively been correlated with the quaternary structure of the protein (*128*).

3. *Miscellaneous*

Pyrococcus furiosus ferredoxin, which contains a single [4Fe–4S] cluster having noncysteinyl ligation on one of its metals, displays in its reduced form a mixture of $S = \frac{1}{2}$ (20%) and $S = \frac{3}{2}$ (80%, with $D = +3.3\ cm^{-1}$, $|E/D| = 0.22$) ground spin states (*130*). Upon binding of cyanide, they are both converted into a new, pure $S = \frac{1}{2}$ state (*131*).

Desulfovibrio africanus ferredoxin III contains one classical [4Fe–4S] cluster and one [3Fe–4S] cluster that can be converted into a [4Fe–4S] cluster having one noncysteinyl ligated metal (*132*). The $S = \frac{3}{2}$ spin state observed in the 8Fe ferredoxin has been attributed to the cluster having one noncysteinyl ligand (*133*).

EPR signals consistent with $S = \frac{3}{2}$ spin states have also been obtained with reduced *C. pasteurianum* hydrogenase I (*134*) and *Clostridium thermoaceticum* CO dehydrogenase (*135*).

E. Room Temperature Data Obtained from Proton NMR

Protons neighboring paramagnetic centers are considerably perturbed by the strong local electronic spin and it is therefore generally easy to distinguish their nuclear magnetic resonances from those of the bulk of the molecule (*89, 136*). These perturbations result in large chemical shifts with strong temperature dependences and short relaxation times, properties that are useful to obtain information on the electronic spin of the paramagnetic center.

This has proved particularly true in the case of the $2[4Fe–4Se]^+$ clostridial ferredoxins (*98*). A set of ~20 resonances, which all integrate to the intensity of one proton, occur outside of the 0- to 10-ppm diamagnetic range. These shifted resonances can be divided into two subsets, each comprising ~8 protons, on the basis of their chemical shifts and temperature dependences. One subset has temperature dependences (~0.2 ppm/K) and chemical shifts very similar to those measured for reduced native ferredoxins. The chemical shifts are slightly larger in the former than in the latter proteins, which is a general effect of the replacement of sulfur by selenium (Section VI). The second set

of resonances displays very different characteristics: the temperature dependence is much larger (up to 1 ppm/K in some cases), and the chemical shifts span a considerably wider range (from -50 to $+160$ ppm). Such features are unprecedented for $[4Fe–4S(e)]^+$ clusters, and most probably reflect the occurrence in the conditions of the NMR experiments, i.e., at room temperature in liquid solution, of electronic spins arising from at least one of the high ground spin states observed in frozen solutions by EPR, Mössbauer, or MCD spectroscopies (Section VII,A). This conclusion has been borne out by measuring the bulk magnetic susceptibility of ferredoxin solutions, which can be derived from the induced chemical shift of a reference proton. The value obtained is related to the effective magnetic moment of the protein and enables a direct comparison between samples (*137*). In the case of reduced *C. pasteurianum* ferredoxin, the seleno derivative exhibits an effective magnetic moment of 6.3 μ_B (Bohr magneton), 50% higher than that (4.2 μ_B) of the native molecule. The large difference observed between the two reduced ferredoxins clearly confirms that the protein containing selenium has an effective spin quantum number at ambient temperature higher than the native one. Thus, the ^1H NMR data demonstrate that at least some of the high-spin states observed at low temperature (<20 K) for reduced $2[4Fe–4Se]^+$ clostridial ferredoxins are still relevant at room temperature, i.e., under conditions in which the protein is functioning.

A completely different situation is encountered in the case of the nitrogenase Fe protein, for which a mixture of $S = \frac{1}{2}$ and $S = \frac{3}{2}$ ground spin states has been evidenced (Section VII,B). The shifted proton resonances of the reduced protein are very similar, with regard to chemical shifts and temperature dependences, to those, among the reduced ferredoxins, which display only $S = \frac{1}{2}$ ground spin states (*115*). Furthermore, the significant spectroscopic features, as well as the solution magnetic susceptibility, are insensitive to variations in solvent compositions, which, at low temperature, considerably modify the relative ratios of the two ground spin states. Binding of adenine nucleotides (ADP, ATP, and some analogs) to the Fe protein induces small changes in the shifted proton resonances (*115*); further discussion of this is outside the scope of this review. Here again, however, the spectroscopic features indicate similar electronic properties of the $[4Fe–4S]^+$ cluster (*115*). It has therefrom been deduced that a single spin manifold of the latter cluster contributes to the paramagnetic shifts of the protons neighboring the active site. This suggests that the ground spin state heterogeneity may arise from constraints appearing upon freezing. Indeed, of the two solvent compositions that induce the most divergent relative abun-

dances of the $S = \frac{1}{2}$ and $S = \frac{3}{2}$ ground spin states, one (50% ethylene glycol) freezes as a glass whereas the other (0.4 *M* urea) is more crystalline. It is relevant to mention here that the EPR spectra of $[2Fe–2S(e)]^+$ synthetic analogs display variations in the main values of their *g* tensors, depending on the solvents in which they are frozen (*93*). Samples of Fe protein prepared with rapid freeze techniques (~5 msec) have been reported to display the spectroscopic signatures of the two ground spin states, but possible changes in the relative proportions of the latter, depending on the rapidity of freezing, have not been indicated (*109*). An experiment has been carried out (*115*) that points to the importance of the freezing process with respect to the ground spin state variability of the Fe protein. EPR samples in several solvent compositions favoring either the $S = \frac{1}{2}$ or the $S = \frac{3}{2}$ spin state were frozen in liquid nitrogen and displayed the expected signals in the expected ratios. The samples were subsequently equilibrated in an acetone–dry ice bath (~230 K), and then taken back to liquid nitrogen temperature (77 K). At no stage in this procedure were the solutions allowed to thaw. The EPR spectra recorded thereafter showed that the relative ratios of the two spin states had changed; for instance, in 0.4 *M* urea, the $S = \frac{1}{2}$ to $S = \frac{3}{2}$ ratio was 1 : 10 before the temperature cycling and 1 : 3 afterward (Fig. 3, spectra a and b). Furthermore, when the samples were thawed and refrozen in liquid nitrogen after the temperature cycling, the ratio returned to the initial 1 : 10 value (Fig. 3, spectrum c). These experiments leave little doubt that the freezing process is of prime importance, in this case at least, for the appearance of the spin state variability and for the modulation of the relative contribution of each of the spin states.

So far, room temperature data are available only for the two protein types discussed above. In the case of the nitrogenase iron protein, facile ground spin state interconversion at cryogenic temperatures correlates with the coalescence at room temperature into a single species, which includes no contribution from the $S = \frac{3}{2}$ ground spin state. In contrast, in the $2[4Fe–4Se]^+$ ferredoxins, the ground spin states are not, despite numerous attempts, interconvertible at low temperature. Moreover, some of these high ground spin states still contribute to the magnetic properties of the reduced Se-substituted ferredoxins in solution. Thus, the active site of the Fe protein appears to be more sensitive to the solvent (directly, or through the polypeptide chain) than those of the clostridial ferredoxins. This inference may be rationalized by the crystal structure of the former protein (*138*), which shows the [4Fe–4S] cluster to be held between the two subunits, in a highly exposed region.

Useful proton NMR spectra are unlikely to be retrieved easily from most of the other proteins discussed in this review, due to their con-

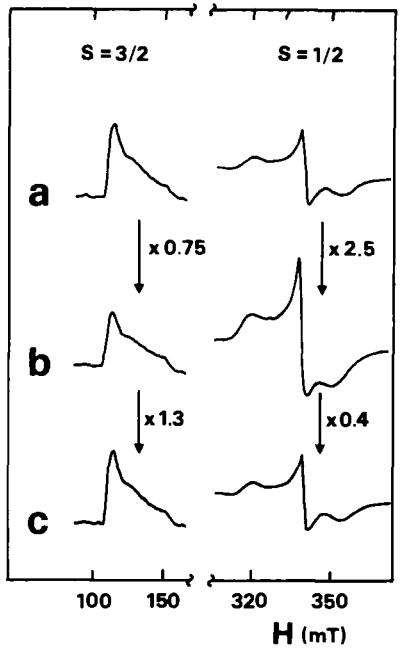

FIG. 3. EPR spectra of *C. pasteurianum* nitrogenase iron protein showing the dependence of the relative amounts of $S = \frac{1}{2}$ and $S = \frac{3}{2}$ spin ground states on the freezing procedure. The protein (30 mg/ml), dissolved in 0.4 *M* urea, 0.05 *M* potassium phosphate, pH 8.0, and 2 m*M* dithionite, was handled and transferred into EPR tubes in an anaerobic glove box (<2 ppm O_2). The tubes were frozen in liquid nitrogen and the spectra were recorded at 5 K for the low-field region and 12 K for the high-field region. Other experimental conditions are given elsewhere (*115*). (a) Spectrum recorded subsequent to initial freezing in liquid nitrogen. (b) Sample (a) brought to acetone/dry ice temperature (230 K) for 15 min. (c) Sample (b) after thawing and subsequent freezing in liquid nitrogen. The numbers next to the arrows are the changes in the integrated intensity of the EPR signals observed after each step in the thermal cycling.

taining paramagnetic centers in addition to those of interest here. *Pyrococcus furiosus* ferredoxin, in view of its small size and single [4Fe–4S] cluster (*130*), might be an exception. A more promising field of investigation is afforded by the synthetic analogs (*117–120*). ^{1}H NMR studies on the host of compounds that have been analyzed in great detail by X-ray crystallography and by low-temperature magnetic techniques might contribute significant data. Previously published NMR spectra, however, including those of some compounds now known to exhibit spin quartet states in frozen solution, consistently display the same features

as those of synthetic clusters and proteins assuming a pure $S = \frac{1}{2}$ ground spin state (*44, 77a, 97, 139*).

F. Significance of the Ground Spin State Variability

The functional relevance of the ground spin state variability of $[4Fe–4S(e)]^+$ clusters may appear doubtful, since 2[4Fe–4Se] ferredoxins are the only case in which they seem to have any bearing on the room temperature electronic properties (Section VII,E). However, these proteins are providing a unique means to explore the rate dependence for electron transfer on electronic structure (and in particular on the spin state) in iron–sulfur proteins. According to current theories (reviewed in Ref. *140*), an electronic factor representing the interactions between the initial and final states of the redox system contributes to the rate of electron transfer. From a detailed comparative survey of the redox reactivity of clostridial ferredoxins with either [4Fe–4S] or [4Fe–4Se] clusters, and for which high-resolution X-ray structures are available (*141, 142*), it should be possible to determine the influence of the initial and final spin states on the redox process.

An additional feature of the ground spin state variability of $[4Fe–4S(e)]^+$ clusters has been the stimulation of intense theoretical work aimed at understanding the electronic structure of the clusters, and in particular the conditions leading to the occurrence of high-spin states. The most recent efforts (*143, 144*) have succeeded, using an appropriate balance of exchange (J) and resonance (B) parameters between the iron atoms, and are able to account for most of the spin states observed and discussed above. Depending on the relative values of the Heisenberg parameters for the Fe(II) pair on one hand, and for the mixed-valence pair on the other hand, the $S = \frac{1}{2}, \frac{3}{2}, \frac{5}{2}$, and $\frac{7}{2}$ (but in no case $\frac{9}{2}$) spin states can occur at lowest energy. Interestingly, the valence localization observed for the $S = \frac{7}{2}$ state (*101*) has been nicely reproduced by the model (*143*).

VIII. Vibrational Spectroscopy of Iron–Selenium Clusters

The properties of metal-containing active sites in proteins indicate small variations that are difficult to detect in X-ray crystal structures. Vibrational spectroscopy has been widely used to characterize these minute changes, as it has the potential to provide a wealth of information on the symmetry and bond strengths of a molecule. Resonance

Raman (RR) spectroscopy, in which laser excitation within an electronic absorption band produces selective enhancement of Raman lines arising from vibrations of the chromophore, is able to reveal specific vibrational features of the active site (*145*).

In the case of iron–sulfur proteins, the instability of the active sites and their poor Raman scattering efficiencies limited information obtainable from early spectra of rubredoxin (*146*) and [2Fe–2S] (*147*) and [4Fe–4S] ferredoxins (*148*). Significant progress has been made by analyzing light scattered by frozen droplets of concentrated solutions of protein (*149*). Application of this experimental approach to iron–sulfur proteins and to synthetic analogs of their active sites has allowed the collection of high-quality spectra (*58, 150–153*) and the measurement of reliable isotopic shifts and depolarization ratios (*58, 154*). A few examples are given below, and these illustrate the wealth of experimental data that can be obtained from the S → Se substitution in iron–sulfur active sites.

A. [2Fe–2Se] Proteins

The first RR study on this type of protein has been carried out on adrenodoxin and on its selenium-substituted analog (*147*). Only three bands assignable to Fe–S(e) stretching frequencies have been detected for the native protein, and two for the selenium-substituted protein. Tentative assignments of the observed bands to Fe–S(cys) and to Fe–S(e)* stretching modes have been derived from the comparison of the spectra (*147*). Later, largely improved RR spectra of another [2Fe–2Se] protein have been obtained: a comprehensive set of data has been collected for spinach ferredoxin, for its Se-substituted analog, and for the [2Fe–2S] ferredoxin from *C. pasteurianum,* including measurements of depolarization ratios, isotopic substitutions on the core chalcogenides (for the spinach ferredoxins), and excitation with several different wavelengths (*154*). The number of bands observed in the Fe–Se stretching frequency range (at least seven in each spectrum), and the high number of totally symmetric modes, have shown that in all of these proteins the chromophores experience distortions lowering their symmetry (*154*) from the D_{2h} point group observed in synthetic analogs (*155*). All bands in the region of 250–450 cm^{-1}, in which the Fe–S stretching modes are expected to occur, display relatively uniform isotopic shifts upon $^{32}S \rightarrow {}^{34}S$ substitution at the core. This suggests an extensive mixing of bridging and terminal motions, hence forbidding assignment of any of the observed bands to simple, normal modes.

In contrast, $^{76}Se \rightarrow {}^{82}Se$ isotopic substitution allows discrimination between the bridging and terminal stretching modes, showing that in this case the coupling between the two types of modes is weaker. In a previous study on spinach ferredoxin and adrenodoxin, inaccurate measurements of $^{32}S \rightarrow {}^{34}S$ isotopic shifts had led to erroneous normal mode calculations and assignments (*155*). Subsequent revisitation of the subject by the same group has yielded data and interpretation (*156*) supporting and extending our former conclusions (*154*).

Analysis of the RR spectra of spinach ferredoxin reconstituted with mixtures of sulfide and selenide has revealed that not only [2Fe–2S] and [2Fe–2Se] clusters but also [2Fe–S–Se] hybrid clusters are present in the reaction products (*48*). Similar occurrences have previously been demonstrated by EPR in the case of adrenodoxin (*82*), and by ^1H NMR for $[Fe_2X_2(SR)_4]^{2-}$ synthetic analogs (*44*).

An extensive set of RR spectra of $[Fe_2X_2(YR)_4]^{2-}$ (X, Y = S, Se) synthetic analogs has been reported, and tentative assignments of the observed bands to bridging or terminal normal modes have been derived from the observed shifts upon S → Se substitution in either one or both positions (*157*). These spectra are valuable in that they display low-frequency bands (in the range of 100–200 cm^{-1}) assignable to bending modes of the Fe–S(e) chromophore. Such bands have also been observed in some spectra of [2Fe–2X] proteins (*152, 154*).

B. [4Fe–4Se] Proteins

RR spectra of Se-substituted *C. pasteurianum* ferredoxin have initially been recorded to analyze the active sites of ferredoxin preparations reconstituted with mixtures of sulfide and selenide. By comparing their spectra with those of proteins containing either chalcogenide alone, they have been shown to contain hybrid clusters of the [4Fe–(4 − *n*)S–*n*Se] series (*153*), similar to those identified in synthetic analogs by ^1H NMR spectroscopy (*44*). Thus, no discrimination between sulfide and selenide occurs when [4Fe–4S(e)] or [2Fe–2S(e)] active sites are inserted into apoferredoxins (see Section III,C). Detailed studies on the synthesis of iron–sulfur clusters have shown that the reaction proceeds in two main steps, the first one being the binding of iron and the second one being the reaction with chalcogenide (*158, 159*). If this reaction scheme holds true for the assembly of active sites in *C. pasteurianum* ferredoxin, our results would suggest that the overall reaction is limited by the binding of iron rather than by the binding of chalcogenide (*43, 153*).

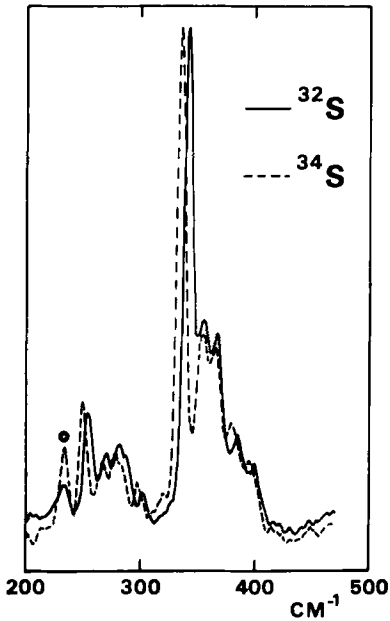

FIG. 4. Resonance Raman spectra of the native (^{32}S) and of the ^{34}S-substituted (on the inorganic sulfur atoms only) 2[4Fe–4S] ferredoxins from *C. pasteurianum*. The preparation of the samples and the experimental conditions have been described (*58*). The excitation wavelength was 457.9 nm. Two bands at 353 and 365 cm^{-1} are practically unshifted, whereas all other bands undergo conspicuous shifts to lower frequency upon ^{34}S substitution. These data have allowed a clear discrimination between the Fe–S* and the Fe–S(cys) stretching modes (*58*). The starred bands arise from the Raman scattering of ice.

RR spectra of 2[4Fe–4S] and 2[4Fe–4Se] *C. pasteurianum* ferredoxins have been analyzed in detail, using isotopic shift measurements upon $^{32}S \rightarrow {}^{34}S$ (Fig. 4) and $^{76}Se \rightarrow {}^{82}Se$ substitutions on the bridging chalcogenides, and determination of the depolarization ratios of most of the observed bands (*58*). Unlike the case of the binuclear clusters (Section VIII,A), the bridging and terminal stretching motions are largely uncoupled whether S or Se is the bridging ligand, thus enabling discrimination between the two types of modes in both cases. Additional data have been obtained with synthetic analogs possessing either aliphatic or aromatic thiolate ligands. This comprehensive set of data has allowed complete assignments to be made for the $Fe_4X_4(Scys)_4$ chromophores in the framework of the D_{2d} point group (*58*), as an extension of previous assignments assuming T_d symmetry (*151*). The subsequent analysis of additional data and normal mode calculations (*160*) confirmed D_{2d} as

the relevant point group for [4Fe–4S(e)] centers in proteins, but challenged some of the previous assignments (*58*).

The comparative analysis of native and Se-substituted active sites has been particularly fruitful in the case of the HiPIP from *C. vinosum*. The $[4Fe–4S(e)]^{2+}$ active sites of the reduced proteins have been demonstrated to display almost the same spectra and thus to assume the same D_{2d} local symmetry as in oxidized *C. pasteurianum* ferredoxin (*40*), in contradiction with a previous report suggesting that the active site of HiPIP experiences smaller distortions than those of low-potential ferredoxins (*160*). These conclusions (*40*) have recently been confirmed by a thorough investigation, including RR data on several ferredoxins and HiPIPs, which has unequivocally shown that the $[4Fe–4S]^{2+}$ clusters in all of the examined proteins display the same distortion from T_d symmetry (*161*). The availability of Se-substituted *C. vinosum* HiPIP has also allowed the vibrational properties of the oxidized $[4Fe–4S(e)]^{3+}$ clusters to be analyzed: the bridging modes are only marginally affected by electron removal, whereas the Fe–S(cys) stretching modes occur at higher frequency than in the reduced protein, and with larger splittings. It has therefore been inferred that the major effect of electron exchange bears on the Fe–S(cys) bonds. One or two of the latter bonds are likely to play a crucial role in the function of these proteins (*40*).

IX. Prospects

Once the feasibility of exchanging the inorganic atoms in the active sites of ferredoxins was established (*34*), it appeared rather trivial to replace sulfide by its close analog selenide. Indeed, the first [2Fe–2Se] ferredoxins were prepared soon thereafter (*25, 36, 37*), although more than a decade elapsed before similar substitutions were carried out in [4Fe–4S] proteins (*39*). Generally, the substitution reactions are rather straightforward, with, in general, hardly any greater experimental difficulties for the assembly of Fe–Se active sites than for Fe–S active sites (Section III,C). It has also turned out that the Se-substituted proteins have most of their properties only marginally modified, as compared to their native counterparts (Sections V and VI).

However, the study of Se-substituted proteins has led to interesting findings. Some of these were targeted; in particular, ^{77}Se ($I = \frac{1}{2}$) was used to demonstrate that the [2Fe–2S(e)] active sites contain two inorganic chalcogenide atoms (*36*), and selenium was implemented as a vibrational band-shifting probe (Section VIII). Other findings have been serendipitous, such as the discovery in clostridial $2[4Fe–4Se]^{+}$ ferredoxins of high ground spin states, which have subsequently been found

to be of widespread occurrence in natural and synthetic $[4Fe–4S(e)]^+$ clusters (Section VII).

These results should encourage further work on chalcogenide substitutions in iron–sulfur proteins. A promising and yet unexplored path is the replacement of sulfur by tellurium, which, if such species can be stabilized, may be expected to yield some further surprises. The successful synthesis of soluble iron–tellurium clusters (Section III,D) suggests the feasibility of their assembly in proteins.

All Se/S substitutions carried out so far have consistently shown an absence of discrimination between the two chalcogenides. This would seem to preclude the selective incorporation of selenide into a subset of atomic positions within an inorganic core. Such site-directed substitutions might nevertheless become possible upon isolation and characterization of enzymatic systems catalyzing the assembly of iron–sulfur clusters into proteins. If such reactions are stepwise, conditions might be found under which a given chalcogenide could be incorporated in predetermined positions, and another one (or an isotope) in the remaining positions. This would allow experimental approaches analogous to those implemented for the iron atoms of aconitase (*162*).

The replacement of sulfur by selenium has been carried out in a number of inorganic cores within iron–sulfur proteins, but not yet on the cysteinyl ligands of these active sites. Selenocysteine has now been incorporated into synthetic peptides having half the size of the smallest ferredoxins (*23*). Since *C. pasteurianum* ferredoxin has been chemically synthesized (*163*), analogs of such proteins with one or several selenocysteinyl ligands to their active sites are likely to be produced in the near future. Another possible way of incorporating selenocysteine into proteins is by chemical modification of serine residues (*20*), although this procedure is likely to raise some problems in the case of ferredoxins, due to their high cysteine content. A major recent advance in the biochemistry of selenium has been the discovery and characterization of an elaborate natural system incorporating selenocysteine in some proteins (Section II,B). Once this reaction mechanism is fully understood, its application to iron–sulfur proteins, by site-directed mutagenesis, could provide an elegant experimental procedure for those proteins that cannot be obtained by total synthesis or chemical modification.

REFERENCES

1. Cotton, F. A., and Wilkinson, G., "Advanced Inorganic Chemistry." Wiley, New York, 1980.
2. Odom, J. D., *Struct. Bonding* **54,** 1 (1983).

3. Frost, D. V., and Ingvoldstad, D., *Chem. Scripta* **8A,** 96 (1975).
4. Doran, J. W., *in* "Advances in Microbial Ecology" (K. C. Marshall, ed.), Vol. 6, p. 1. Plenum, New York, 1982.
5. Spallholz, J. E., Martin, J. L., and Ganther, H. E., eds., *in* "Selenium in Biology and Medicine." Avi Publ., Westport, Connecticut, 1981.
6. Schwarz, K., and Foltz, C. M., *J. Am. Chem. Soc.* **79,** 3292 (1957).
7. Diplock, A. T., *Philos. Trans. R. Soc. London, Ser. B* **294,** 105 (1981).
8. Stadtman, T. C., *Annu. Rev. Biochem.* **59,** 111 (1990).
9. Brown, T. A., and Schrift, A., *Biol. Rev.* **57,** 59 (1982).
10. Behne, D., Kyriakopoulos, A., Meinhold, H., and Köhrle, J., *Biochem. Biophys. Res. Commun.* **173,** 1143 (1990).
11. Berry, M. J., Banu, L., and Larsen, P. R., *Nature (London)* **349,** 438 (1991).
12. Hill, K. E., Lloyd, R. S., Yang, J.-G., Read, R., and Burk, R. F. *J. Biol. Chem.* **266,** 10050 (1991).
13. Chambers, I., Frampton, J., Goldfarb, P., Affara, N., McBain, W., and Harrison, P. R., *EMBO J.* **5,** 1221 (1986).
14. Zinoni, F., Birkmann, A., Stadtman, T. C., and Böck, A., *Proc. Natl. Acad. Sci. U.S.A.* **83,** 4650 (1986).
15. Sunde, R. A., *Annu. Rev. Nutr.* **10,** 451 (1990).
16. Stadtman, T. C., *Science* **183,** 915 (1974).
17. Huber, R. E., and Criddle, R. S., *Biochim. Biophys. Acta* **141,** 587 (1967).
18. Tsen, C. C., and Tappel, A. L., *J. Biol. Chem.* **233,** 1230 (1958).
19. Kice, J. L., Lee, T. W. S., and Pan, S.-T., *J. Am. Chem. Soc.* **102,** 4448 (1980).
20. Wu, Z.-P., and Hilvert, D., *J. Am. Chem. Soc.* **111,** 4513 (1989).
20a. Wu, Z.-P., and Hilvert, D., *J. Am. Chem. Soc.* **112,** 5647 (1990).
21. Walter, R., and Chan, W. Y., *J. Am. Chem. Soc.* **89,** 3892 (1967).
22. Hartrodt, B., Neubert, K., Bierwolf, B., Blech, W., and Jakubke, H.-D., *Tetrahedron Lett.* **21,** 2393 (1980).
23. Oikawa, T., Esaki, N., Tanaka, H., and Soda, K., *Proc. Natl. Acad. Sci. U.S.A.* **88,** 3057 (1991).
24. Frank, P., Licht, A., Tullius, T. D., Hodgson, K. O., and Pecht, I., *J. Biol. Chem.* **260,** 5518 (1985).
25. Yang, W., Hendrickson, W. A., Kalman, E. T., and Crouch, R. J., *J. Biol. Chem.* **265,** 13553 (1990).
26. Weatherill, T. D., Rauchfuss, T. B., and Scott, R. A., *Inorg. Chem.* **25,** 1466 (1986).
27. Eidsness, M. K., Scott, R. A., Prickril, B. C., DerVartanian, D. V., LeGall, J., Moura, I., Moura, J. J. G., and Peck, H. D., Jr., *Proc. Natl. Acad. Sci. U.S.A.* **86,** 147 (1989).
28. Yang, W., Hendrickson, W. A., Crouch, R. J., and Satow, Y., *Science* **249,** 1398 (1990).
29. He, S. H., Teixeira, M., LeGall, J., Patil, D. S., Moura, I., Moura, J. J. G., DerVartanian, D. V., Huynh, B. H., and Peck, H. D., Jr., *J. Biol. Chem.* **264,** 2678 (1989).
30. Mullen, G. P., Dunlap, R. B., and Odom, J. D., *J. Am. Chem. Soc.* **107,** 7187 (1985).
31. Gettins, P., and Crews, B. C., *J. Biol. Chem.* **266,** 4804 (1991).
32. Mortenson, L. E., Valentine, R. C., and Carnahan, J. E., *Biochem. Biophys. Res. Commun.* **7,** 448 (1962).
33. Tagawa, K., and Arnon, D. I., *Nature (London)* **195,** 537 (1962).
34. Malkin, R., and Rabinowitz, J. C., *Biochem. Biophys. Res. Commun.* **23,** 822 (1966).
34a. Hong, J.-S., and Rabinowitz, J. C., *Biochem. Biophys. Res. Commun.* **29,** 246 (1967).

35. Tsibris, J. C. M., Namtvedt, M. J., and Gunsalus, I. C., *Biochem. Biophys. Res. Commun.* **30,** 323 (1968).
36. Orme-Johnson, W. H., Hansen, R. E., Beinert, H., Tsibris, J. C. M., Bartholomaus, R. C., and Gunsalus, I. C., *Proc. Natl. Acad. Sci. U.S.A.* **60,** 368 (1968).
37. Fee, J. A., and Palmer, G., *Biochim. Biophys. Acta* **245,** 175 (1971).
38. Sugiura, Y., Ishizu, K., and Kimura, T., *Biochemistry* **14,** 97 (1975).
39. Meyer, J., and Moulis, J.-M., *Biochem. Biophys. Res. Commun.* **103,** 667 (1981).
40. Moulis, J.-M., Lutz, M., Gaillard, J., and Noodleman, L., *Biochemistry* **27,** 8712 (1988).
41. Surerus, K. K., Kennedy, M. C., Beinert, H., and Münck, E., *Proc. Natl. Acad. Sci. U.S.A.* **86,** 9846 (1989).
42. Hong, J.-S., and Rabinowitz, J. C., *J. Biol. Chem.* **245,** 6582 (1970).
43. Moulis, J.-M., and Meyer, J., *Biochemistry* **21,** 4762 (1982).
44. Reynolds, J. G., and Holm, R. H., *Inorg. Chem.* **20,** 1873 (1981).
45. Petering, D., Fee, J. A., and Palmer, G., *J. Biol. Chem.* **246,** 643 (1971).
46. Wood, J. L., *in* "Methods in Enzymology" (W. B. Jakoby and O. Griffith) Vol. 143, p. 25. Academic Press, New York, 1987.
47. Rao, K. K., Cammack, R., Hall, D. O., and Johnson, C. E., *Biochem. J.* **122,** 257 (1971).
48. Meyer, J., Moulis, J.-M., and Lutz, M., *Biochim. Biophys. Acta* **871,** 243 (1986).
49. Gaillard, J., Moulis, J.-M., Auric, P., and Meyer, J., *Biochemistry* **25,** 464 (1986).
50. Kennedy, M. C., and Beinert, H., *J. Biol. Chem.* **263,** 8194 (1988).
51. Que, L., Jr., Holm, R. H., and Mortenson, L. E., *J. Am. Chem. Soc.* **97,** 463 (1975).
52. Bonomi, F., and Kurtz, D. M., Jr., *Anal. Biochem.* **142,** 226 (1984).
53. Orme-Johnson, W. H., and Holm, R. H., *in* "Methods in Enzymology" (S. Fleischer and L. Packer, eds.), Vol. 53, p. 268. Academic Press, New York, 1978.
54. Waitkins, G. R., and Shutt, R., *Inorg. Synth.* **2,** 183 (1946).
55. Nitsche, R., *Angew. Chem.* **69,** 333 (1957).
56. Klayman, D. L., and Griffin, T. S., *J. Am. Chem. Soc.* **95,** 197 (1973).
57. Fee, J. A., Mayhew, S. G., and Palmer, G., *Biochim. Biophys. Acta* **245,** 196 (1971).
58. Moulis, J.-M., Meyer, J., and Lutz, M., *Biochemistry* **23,** 6605 (1984).
59. Moulis, J.-M., *Ph.D. Thesis,* University of Grenoble, Grenoble, France (1985).
60. Klemm, W., Sodomann, H., and Langmesser, P., *Z. Anorg. Allg. Chem.* **241,** 281 (1939).
61. Bronger, W., Kimpel, M., and Schmitz, D., *Angew. Chem., Int. Ed. Engl.* **21,** 544 (1982).
62. Arakawa, S., and Kimura, T., *Biochim. Biophys. Acta* **580,** 382 (1979).
63. Simon, W., Wilk, A., Krebs, B., and Henkel, G., *Angew. Chem., Int. Ed. Engl.* **26,** 1009 (1987).
63a. Krebs, B., and Henkel, G., *Angew. Chem., Int. Ed. Engl.* **30,** 769 (1991).
64. Barbaro, P., Bencini, A., Bertini, I., Briganti, F., and Midollini, S., *J. Am. Chem. Soc.* **112,** 7238 (1990).
65. Hausinger, R. P., *BioFactors* **2,** 179 (1990).
66. Hall, D. O., Cammack, R., and Rao, K. K., *Nature (London)* **233,** 136 (1971).
67. Sugiura, Y., Ishizu, K., and Kimura, T., *Biochem. Biophys. Res. Commun.* **60,** 334 (1974).
68. Christou, G., Ridge, B., and Rydon, H. N., *J. Chem. Soc., Chem. Commun.* p. 20 (1979).
69. Pagani, S., Bonomi, F., and Cerletti, P., *Eur. J. Biochem.* **142,** 361 (1984).
70. Bonomi, F., Pagani, S., and Kurtz, D. M., Jr., *Eur. J. Biochem.* **148,** 67 (1985).

71. Sandberg, W., Graves, M. C., and Rabinowitz, J. C., *Trends Biochem. Sci.* **12,** 56 (1987).
72. Takahashi, Y., Mitsui, A., Hase, T., and Matsubara, H., *Proc. Natl. Acad. Sci. U.S.A.* **83,** 2434 (1986).
73. Takahashi, Y., Mitsui, A., Fujita, Y., and Matsubara, H., *Plant Physiol.* **95,** 104 (1991).
74. Dean, D. R., and Jacobson, M. R., *in* "Nitrogen Fixation" (G. Stacey, R. H. Burris, and H. J. Evans, eds.), p. 759. Chapman & Hall, London, 1991.
75. Voordouw, G., Hagen, W. R., Krüse-Wolters, K. M., van Berkel-Arts, A., and Veeger, C., *Eur. J. Biochem.* **162,** 31 (1987).
76. Meyer, J., Bruschi, M. H., Bonicel, J. J., and Bovier-Lapierre, G. E., *Biochemistry* **25,** 6054 (1986).
77. Bobrik, M. A., Laskowski, E. J., Johnson, R. W., Gillum, W. O., Berg, J. M., Hodgson, K. O., and Holm, R. H., *Inorg. Chem.* **17,** 1402 (1978).
77a. Yu, S.-B., Papaefthymiou, G. C., and Holm, R. H., *Inorg. Chem.* **30,** 3476 (1991).
78. Maskiewicz, R., and Bruice, T. C., *Biochemistry* **16,** 3024 (1977).
79. Reynolds, J. G., and Holm, R. H., *Inorg. Chem.* **19,** 3257 (1980).
80. Christou, G., Ridge, B., and Rydon, H. N., *J. Chem. Soc., Chem. Commun.,* 1423 (1978).
81. Wilson, G. S., Tsibris, J. C. M., and Gunsalus, I. C., *J. Biol. Chem.* **248,** 6059. (1973).
82. Mukai, K., Huang, J. J., and Kimura, T., *Biochim. Biophys. Acta* **336,** 427 (1974).
83. Cammack, R., *in* "Charge and Field Effects in Biosystems" (M. J. Allen and P. N. R. Usherwood, eds.), p. 41. Abacus Press, Tunbridge Wells, U.K., 1984.
84. Beinert, H., and Sands, R. H., *Biochem. Biophys. Res. Commun.* **3,** 41 (1960).
85. Brintzinger, H., Palmer, G., and Sands, R. H., *Proc. Natl. Acad. Sci. U.S.A.* **55,** 397 (1966).
86. Gibson, J. F., Hall, D. O., Thornley, J. H. M., and Whatley, F. R., *Proc. Natl. Acad. Sci. U.S.A.* **56,** 987 (1966).
87. Cammack, R., Dickson, D. P. E., and Johnson, C. E., *in* "Iron-Sulfur Proteins" (W. Lovenberg, ed.), Vol. 3, p. 283. Academic Press, New York, 1977.
88. Johnson, M. K., Robinson, A. E., and Thomson, A. J., *in* "Iron-Sulfur Proteins" (T. G. Spiro, ed.), p. 367. Wiley (Interscience), New York, 1982.
89. Phillips, W. D., and Poe, M., *in* "Iron-Sulfur Proteins" (W. Lovenberg, ed.), Vol. 2, p. 255. Academic Press, New York, 1973.
90. Sands, R. H., and Dunham, W. R., *Q. Rev. Biophys.* **7,** 443 (1975).
91. Bertrand, P., and Gayda, J.-P., *Biochim. Biophys. Acta* **579,** 107 (1979).
92. Fee, J. A., Findling, K. L., Yoshida, T., Hille, R., Tarr, G. E., Hearshen, D. O., Dunham, W. R., Day, E. P., Kent, T. A., and Münck, E., *J. Biol. Chem.* **259,** 124 (1984).
93. Beardwood, P., and Gibson, J. F., *J. Chem. Soc., Dalton Trans.,* 737 (1983).
94. Münck, E., Debrunner, P. G., Tsibris, J. C. M., and Gunsalus, I. C., *Biochemistry* **11,** 855 (1972).
95. Bowman, M., Kevan, L., Mukai, K., and Kimura, T., *Biochim. Biophys. Acta* **328,** 244 (1973).
96. Bertrand, P., and Gayda, J.-P., *Biochim. Biophys. Acta* **625,** 337 (1980).
97. Reynolds, J. G., Coyle, C. L., and Holm, R. H., *J. Am. Chem. Soc.* **102,** 4350 (1980).
98. Gaillard, J., Moulis, J.-M., and Meyer, J., *Inorg. Chem.* **26,** 320 (1987).
99. George, S. J., Thomson, A. J., Crabtree, D. E., Meyer, J., and Moulis, J.-M., *New J. Chem.* **15,** 455 (1991).

100. Moulis, J.-M., Auric, P., Gaillard, J., and Meyer, J., *J. Biol. Chem.* **259,** 11396 (1984).
101. Auric, P., Gaillard, J., Meyer, J., and Moulis, J.-M., *Biochem. J.* **242,** 525 (1987).
102. Rius, G., and Lamotte, B., *J. Am. Chem. Soc.* **111,** 2464 (1989).
103. Sola, M., Cowan, J. A., and Gray, H. B., *J. Am. Chem. Soc.* **111,** 6627 (1989).
104. Laskowski, E. J., Reynolds, J. G., Frankel, R. B., Foner, S., Papaefthymiou, G. C., and Holm, R. H., *J. Am. Chem. Soc.* **101,** 6562 (1978).
104a. Collison, D., and Mabbs, F. E., *J. Chem. Soc., Dalton Trans.*, 1565 (1982).
105. Zimmermann, R., Münck, E., Brill, W. J., Shah, V. K., Henzl, M. T., Rawlings, J., and Orme-Johnson, W. H., *Biochim. Biophys. Acta* **537,** 185 (1978).
106. Vollmer, S. J., Switzer, R. L., and Debrunner, P. G., *J. Biol. Chem.* **258,** 14284 (1983).
107. Mathews, R., Charlton, S., Sands, R. H., and Palmer, G., *J. Biol. Chem.* **249,** 4326 (1974).
108. Orme-Johnson, W. H., *Annu. Rev. Biophys. Biophys. Chem.* **14,** 419 (1985).
109. Lindahl, P. A., Day, E. P., Kent, T. A., Orme-Johnson, W. H., and Münck, E., *J. Biol. Chem.* **260,** 11160 (1985).
110. Zumft, W. G., Palmer, G., and Mortenson, L. E., *Biochim. Biophys. Acta* **292,** 413 (1973).
111. Lindahl, P. A., Gorelick, N. J., Münck, E., and Orme-Johnson, W. H., *J. Biol. Chem.* **262,** 14945 (1987).
112. Watt, G. D., and McDonald, J. W., *Biochemistry* **24,** 7226 (1985).
113. Hagen, W. R., Eady, R. R., Dunham, W. R., and Haaker, H., *FEBS Lett.* **189,** 250 (1985).
114. Morgan, T. V., Prince, R. C., and Mortenson, L. E., *FEBS Lett.* **206,** 4 (1986).
115. Meyer, J., Gaillard, J., and Moulis, J.-M., *Biochemistry* **27,** 6150 (1988).
116. Holm, R. H., Ciurli, S., and Weigel, J. A., *Prog. Inorg. Chem.* **38,** 1 (1990).
117. Carney, M. J., Holm, R. H., Papaefthymiou, G. C., and Frankel, R. B., *J. Am. Chem. Soc.* **108,** 3519 (1986).
118. Carney, M. J., Papaefthymiou, G. C., Spartalian, K., Frankel, R. B., and Holm, R. H., *J. Am. Chem. Soc.* **110,** 6084 (1988).
119. Carney, M. J., Papaefthymiou, G. C., Whitener, M. A., Spartalian, K., Frankel, R. B., and Holm, R. H., *Inorg. Chem.* **27,** 346 (1988).
120. Carney, M. J., Papaefthymiou, G. C., Frankel, R. B., and Holm, R. H., *Inorg. Chem.* **28,** 1497 (1989).
120a. Bolin, J. T., Campobasso, N., Muchmore, S. W., Minor, W., Mortenson, L. E., and Morgan, T. V., Abstract K004, Fifth International Conference on Bioinorganic Chemistry, Oxford, 1991.
121. McLean, P. A., Papaefthymiou, V., Orme-Johnson, W. H., and Münck, E., *J. Biol. Chem.* **262,** 12900 (1987).
122. Johnson, M. K., Thomson, A. J., Robinson, A. E., and Smith, B. E., *Biochim. Biophys. Acta* **671,** 61 (1981).
123. Smith, J. P., Emptage, M. H., and Orme-Johnson, W. H., *J. Biol. Chem.* **257,** 2310 (1982).
124. Hagen, W. R., Wassink, H., Eady, R. R., Smith, B. E., and Haaker, H., *Eur. J. Biochem.* **169,** 457 (1987).
125. Lindahl, P. A., Papaefthtymiou, V., Orme-Johnson, W. H., and Münck, E., *J. Biol. Chem.* **263,** 19412 (1988).
126. Switzer, R. L., *BioFactors* **2,** 77 (1989).
127. Grandoni, J. A., Switzer, R. L., Makaroff, C. A., and Zalkin, H., *J. Biol. Chem.* **264,** 6058 (1989).

128. Oñate, Y. A., Vollmer, S. J., Switzer, R. L., and Johnson, M. K., *J. Biol. Chem.* **264,** 18386 (1989).
129. Wong, J. Y., Meyer, E., and Switzer, R. L., *J. Biol. Chem.* **252,** 7424 (1977).
130. Conover, R. C., Kowal, A. T., Fu, W., Park, J.-B., Aono, S., Adams, M. W. W., and Johnson, M. K., *J. Biol. Chem.* **265,** 8533 (1990).
131. Conover, R. C., Park, J.-B., Adams, M. W. W., and Johnson, M. K., *J. Am. Chem. Soc.* **113,** 2799 (1991).
132. Armstrong, F. A., George, S. J., Cammack, R., Hatchikian, E. C., Thomson, A. J., *Biochem. J.* **264,** 265 (1989).
133. George, S. J., Armstrong, F. A., Hatchikian, E. C., and Thomson, A. J., *Biochem. J.* **264,** 275 (1989).
134. Zambrano, I. C., Kowal, A. T., Mortenson, L. E., Adams, M. W. W., and Johnson, M. K., *J. Biol. Chem.* **264,** 20974 (1989).
135. Lindahl, P. A., Münck, E., and Ragsdale, S. W., *J. Biol. Chem.* **265,** 3873 (1990).
136. La Mar, G. N., *in* "Biological Applications of Magnetic Resonance" (R. G. Shulman, ed.), p. 305. Academic Press, New York, 1979.
137. Phillips, W. D., and Poe, M., *in* "Methods in Enzymology" (A. S. Pietro, ed.), Vol. 24, p. 304. Academic Press, New York, 1972.
138. Georgiadis, M. M., Chakrabarti, P., and Rees, D. C., *in* "Nitrogen Fixation: Achievements and Objectives" (P. M. Gresshoff, L. E. Roth, G. Stacey, and W. E. Newton, eds.), p. 111. Chapman & Hall, New York, 1990.
139. Reynolds, J. G., Laskowski, E. J., and Holm, R. H., *J. Am. Chem. Soc.* **100,** 5315 (1978).
140. Bertrand, P., *Struct. Bonding* **75,** 1 (1991).
141. Adman, E. T., Sieker, L. C., and Jensen, L. H., *J. Biol. Chem.* **251,** 3801 (1976).
142. Tranqui, D., Fanchon, E., Vicat, J., Sieker, L. C., Meyer, J., Moulis, J.-M., Gagnon, J., and Duée, E. D., Abstract D049, Fifth International Conference on Bioinorganic Chemistry, Oxford, 1991.
143. Noodleman, L., *Inorg. Chem.* **30,** 246 (1991).
144. Noodleman, L., *Inorg. Chem.* **30,** 256 (1991).
145. Meyer, J., Moulis, M., and Lutz, M., *in* "Frontiers in Bioinorganic Chemistry" (A. V. Xavier, ed.), p. 537. VCH Verlag, Weinheim, 1986.
146. Long II, T. V., and Loehr, T. M., *J. Am. Chem. Soc.* **92,** 6384 (1970).
147. Tang, S.-P. W., Spiro, T. G., Mukai, K., and Kimura, T., *Biochem. Biophys. Res. Commun.* **53,** 869 (1973).
148. Tang, S.-P. W., Spiro, T. G., Antanaitis, C., Moss, T. H., Holm, R. H., Herskovitz, T., and Mortenson, L. E., *Biochem. Biophys. Res. Commun.* **62,** 1 (1975).
149. Lutz, M., *Biochim. Biophys. Acta* **460,** 408 (1977).
150. Lutz, M., Moulis, J.-M., and Meyer, J., *FEBS Lett.* **163,** 212 (1983).
151. Johnson, M. K., Czernuszewicz, R. S., Spiro, T. G., Fee, J. A., and Sweeney, W. V., *J. Am. Chem. Soc.* **105,** 6671 (1983).
152. Meyer, J., Moulis, J.-M., and Lutz, M., *Biochem. Biophys. Res. Commun.* **119,** 828 (1984).
153. Moulis, J.-M., Meyer, J., and Lutz, M., *Biochem. J.* **219,** 829 (1984).
154. Meyer, J., Moulis, J.-M., and Lutz, M., *Biochim. Biophys. Acta* **873,** 108 (1986).
155. Yachandra, V. K., Hare, J., Gewirth, A., Czernuszewicz, R. S., Kimura, T., Holm, R. H., and Spiro, T. G., *J. Am. Chem. Soc.* **105,** 6462 (1983).
156. Han, S., Czernuszewicz, R. S., Kimura, T., Adams, M. W. W., and Spiro, T. G., *J. Am. Chem. Soc.* **111,** 3505 (1989).
157. Beardwood, P., and Gibson, J. F., *J. Chem. Soc., Dalton Trans.,* 1507 (1984).

158. Christou, G., Ridge, B., and Rydon, H. N., *J. Chem. Soc., Chem. Commun.*, 908 (1977).

159. Hagen, K. S., Reynolds, J. G., and Holm, R. H., *J. Am. Chem. Soc.* **103,** 4054 (1981).

160. Czernuszewicz, R. S., Macor, K. A., Johnson, M. K., Gewirth, A., and Spiro, T. G., *J. Am. Chem. Soc.* **109,** 7178 (1987).

161. Backes, G., Mino, Y., Loehr, T. M., Meyer, T. E., Cusanovich, M. A., Sweeney, W. V., Adman, E. T., and Sanders-Loehr, J., *J. Am. Chem. Soc.* **113,** 2055 (1991).

162. Beinert, H., and Kennedy, M. C., *Eur. J. Biochem.* **186,** 5 (1989).

163. Smith, E. T., Feinberg, B. A., Richards, J. H., and Tomich, J. M., *J. Am. Chem. Soc.* **113,** 688 (1991).